Addis Ababa University

Addis Ababa Institute of Technology

School of Mechanical and Industrial Engineering

Numerical Analysis of the Effect of Surface Finish and Material Properties on the Carburized Moly Based Low Alloy Material Subjected to A Contact Load

---

By

Yibeltal Ali Bahru

October, 2022

Addis Ababa, Ethiopia

Addis Ababa University

Addis Ababa Institute of Technology

School of Mechanical and Industrial Engineering

Numerical Analysis of the Effect of Surface Finish and Material Properties on the Carburized Moly Based Low Alloy Material Subjected to A Contact Load By

Yibeltal Ali Bahru

A Thesis Submitted to Graduate School of Addis Ababa University (AAU) for the Partial Fulfillment of Degree of Masters of Science (M.Sc.) in Mechanical Engineering (Applied Mechanics).

Advisor: Behailu Mamo (Ph.D. Candidate)

October, 2022

Addis Ababa, Ethiopia

Letter of Certification

Addis Ababa University

Addis Ababa Institute of Technology

School of Graduate Studies

This is to certify that the thesis prepared by Yibeltal Ali Bahru entitled "*Numerical Analysis of the Effect of Surface Finish and Material Properties on the Carburized Moly Based Low Alloy Material Subjected to A Contact Load*" in partial fulfillment of the requirements for the degree of Masters of Science in Mechanical Engineering (Applied Mechanics) compiles with the regulation of Addis Ababa University and meets the accepted standards concerning originality and quality.

Board of Examining Committee:

Behailu Mamo (Ph.D Candidate) Signature: _____ Date: _____

Advisor:

Haileleoul Sahle (Ph.D) Signature: _____ Date: _____

External examiner:

Mulugeta (Ph.D) Signature: _____ Date: _____

Internal examiner:

Araya (Ph.D) Signature: _____ Date: _____

Chair of Department

Declaration

I, the under signed, declare that this thesis is the result of my work and that all sources or materials used for this thesis have been dually acknowledged. This work is submitted in partial fulfillment of the requirements for a Master's Degree in Mechanical engineering (Applied Mechanics) at Addis Ababa University, Addis Ababa Institute of Technology, School of Mechanical and Industrial Engineering. I certainly declare that this thesis has not been submitted to any other institution anywhere for the award of any academic degree, diploma, and/or certificate.

Yibeltal Ali Bahiru Signature: _____ Date: _____

This is to certify that the above declaration made by the candidate is correct to the best of my knowledge.

Advisor: Behailu Mamo (Ph.D. Candidate) Signature: _____ Date: _____

Acknowledgment

Glory be to the Father, and to the Son, and to the Holy Spirit, one God; for his immeasurable love and guidance in what had seemed like an insurmountable journey, Amen! My veneration and gratitude to the Holy Virgin Saint Merry, for lifting me up in every bit of this journey and for making the path brighter.

I express my sincere appreciation to my Advisor Behailu Mamo (Ph.D. Candidate) for the useful comments, remarks and, encouragement throughout this thesis work.

To my families, for your incessant assistantship in every aspect of my life, for believing in me, and for inheriting the discipline and meticulousness, no words would be enough to describe how thankful I am. May God bless you with long life and health. To my friends, thank you for your support, advice and for giving me strength throughout my journey in many different ways.

Furthermore, I like to thank my peers in the class and at the campus, who have shared their support and precious time during many lively technical discussions about the thesis.

Abstract

Contact between rough surfaces between surfaces affects a variety of phenomena including friction, wear, thermal contact resistance, and electrical contact resistance. Different studies done on the mechanics of contacting bodies using analytical and experimental methods. Even though the experimental method to determine the surface treatment parameters is convenient and effective, the method is very expensive, consume more time to complete and it needs advanced tools. Furthermore, the analytical methods in analyzing real surface topography is a simplifying approach, which has low accuracy. Therefore, numerical modeling of the contact between rough surfaces is the alternative method. the aim of the study was to model the contact pressure contacting bodies to determine the effect of material density variation and surface finish method (machined and powder metallurgy surface) using finite element analysis utilizing ABAQUS software. The plastic contact of a rough surface and smooth flat surface is analyzed by modeling the rough surface as an isotopic, Gaussian, and random process. For running FE analysis an interface MATLAB code and Solid work software were used to create a 3D model from the measurement data. To achieve the objectives of the study particular material were selected and data were collected and rough surface modeling using computational model were performed. Result of the study in terms of contact load, real area of contact, and contact pressure are extracted from each contact analysis depicted that, the low-density PM rough surface leads to minimum area of contact but attains the maximum value of contact pressure $P_{\max}$ *and cross hardness limit earlier when compared with the low-density machined and high-density PM rough surface. In the PM surface model, the* $P_{\max}/Y$ *ratio to cross the hardness limit of 2.22 at* $P_n/A_n E$ *of 0.0042 and in the machined surface model the* $P_{\max}/Y$ *ratio to cross the hardness limit of 2.22 at* $P_n/A_n E$ *of 0.0057. The area of contact decrease whereas the* P_{mean} *and* $P_{\max}$ *increases with a decrease in density value. In the machined surfaces, the contact load is shared by most of the contacting asperities and the asperity interactions restrain the asperities to remain in elastic state mostly even at high loads relative to PM surfaces. The real contact area is low and the von mises stresses and contact pressure are high for the low-density surface as compared to high-density surface, for the surface with* $\rho = 7.35 g/cm^3$*, real contact area occurs at* $0.6377 mm^2$ *or 10.2% of nominal contact area, for the surface with* $\rho = 7.35 g/cm^3$*, real contact area occurs at* $1.14115\ mm^2$ *or 18.25% of nominal contact area.*

Key words: *Numerical Analysis, Surface Finish, Carburized Moly Based Low Alloy Material, Contact Load*

Table of Contents

List of Abbreviations

Ra	Average roughness	[mm]
N	Number of asperities in one surface	[-]
L_c	Sample length or cutoff length	[mm]
2b	Contact width	[mm]
μ	Mean	[mm]
σ^2	Variance	[mm^2]
p_t	Real pressure	[MPa]
p_n	Apparent pressure	[MPa]
A_t	Real area of contact	[mm^2]
A_n	Apparent area	[mm^2]
ρ	Density	[g/cm^3]
P	Pressure distribution	[MPa]
Po	Hertzian pressure	[MPa]
E	Elastic modulus	[MPa]
Y	Yield strength	[MPa]
H	Hardness	[MPa]
P_{max}	Maximum contact pressure	[MPa]
P_{mean}	Maximum contact pressure	[MPa]
υ	Poisson's ratio	[-]
W	Applied load	[N]

Nomenclatures

ACF	Autocorrelation function
C3D6	Six node wedge element
CAD	Computer aided drawing
CAE	Computer-aided engineering
CLA	Centre line average
FEM	Finite element method
FEMAP	Finite Element Modeling and Postprocessing
FFT	Fast Fourier transform
GHD	Gaussian height distribution
IFFT	Inverse fast Fourier transform
MEMS	Micro electromechanical systems
PDF	Probability density function
PM	Powder Metallurgy
PSD	Power spectral density
RMS	Root mean square

List of Figures

List of Tables

Chapter 1: Introduction

1.1 Background of the Study

Tribology is the science and technology of two interacting surfaces in relative motion, and related subjects and practices. Even though the history of tribology goes back to 2600 B.C, a significant impact of tribology applied to machinery production during the industrial revolution in the ninetieth century. The enormous industrial growth led to the demand for a better understanding of tribology. Finally, modern tribology has seen areas such as bio-tribology and Nano-tribology emerge and the subject continues to play a significant role in manufacturing [1].

Tribology studies the different fields including contact mechanics which is the fundamental one since it studies the interaction of solid surfaces. The interaction or contact of surface bodies can occur on many different scales, ranging from nanoscale asperities up to tires on roads and even contact between tectonic plates. Contact between solids is undeniably important because it is such a common and critical occurrence in our daily lives, health, industry, and even on the scale of heavenly bodies and the universe [2].

When viewed under the proper magnification, all surfaces exhibit some roughness or deviation from being perfectly smooth. Some surfaces, on the other hand, appear rough even when no magnification is used. Regardless of scale roughness will induce, contact between surfaces to occur at the peaks and make accurate modeling difficult. This roughness frequently appears on multiple scales rather than just one. As a result, describing the geometry of surfaces in detail is extremely difficult [2].

Despite the difficulty of describing surface roughness, the contact between rough surfaces affects a variety of phenomena in our environment, including friction, wear, thermal contact resistance, and electrical contact resistance. As a result, being able to make at least reasonable predictions of the pressure and real area of contact between two contacting rough surfaces is critical [2].

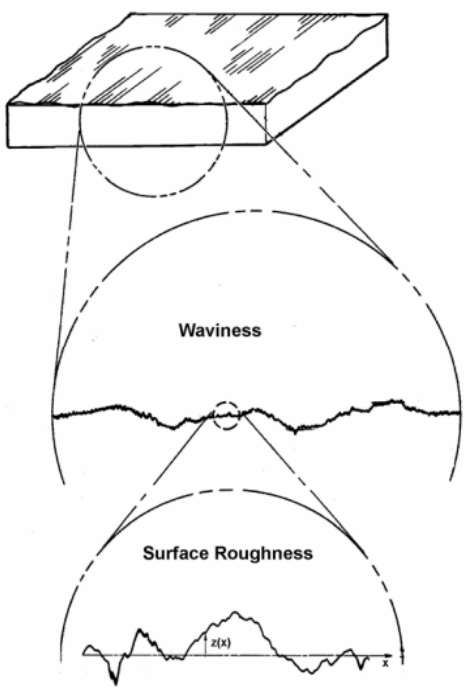

Figure 1.1: Illustration of self-affine property of surface roughness [3]

The transmission of load from one rubbing surface to its mating surface under dry contact or boundary lubrication is an important study area in mechanical engineering. Regardless of whether the surfaces are conformal, such as lathe support or a journal in a sleeve bearing, or counter formal, such as two mating convex gear teeth, cams, and tappets, or rolling elements on their raceways, the transmission of the load is associated with the concentration of the contact pressure. Because of the surface roughness, contact with conformal surfaces will be limited to, or near to, the peaks of the highest asperities, and hence will be distributed. Even if the surface of the counter formal is perfectly smooth, the contact will tend to concentrate [4].

The morphology of the surface is scale-dependent. Surface morphology can be classified as surface roughness, waviness, and lay at the micrometer, millimeter, and meter scales in many engineering applications [3]. In manufacturing engineering, surface finish is an important parameter that can affect the performance of component as well as the cost of production. The surface polish of the components in question has been implicated for a variety of failures, some of which were catastrophic and resulted in high costs [5]. The cam function is heavily influenced by the final manufacturing procedures. It's also a complicated system with a large variety of failure modes [2].

The mechanical and surface properties are essential for the characterization of materials. The requirement of products with good quality in terms of high strength, good surface finish, lower cost,

and less environmental effects is the challenge of the manufacturing industries. The roughness of surfaces is considered an essential parameter in the manufacturing of mechanical parts like cam and follower because it is an indication of the surface quality of the machined parts. Controlling the machining process like cutting speed, depth of cut and feed rate can improve the final surface quality of a product [6].

The contact between the two surfaces is critical, especially studies related to wear are critical for the better functionality and efficiency of the cam system. Most of the wear mechanisms are strongly linked to the pressure between the two surfaces in contact. Different studies are done on the contact mechanics of the cam and follower by using experimental methods. Even though the experimental method to determine the surface treatment method parameters is convenient and effective, the method is very expensive because it takes some time to complete and it needs advanced tools. The analytical method can be implemented using mathematical equations. The analytical method in analyzing real surface topography has a limitation in that it can only be used with a simple model to represent an asperity, such as a spherical geometry model. The accuracy of the results will be impacted by this simplifying approach.

However, the finite element (FE) model offers a promising option for modeling the real surface roughness, and the result provides much better as compared to experimental and analytical methods [14,15]. Therefore, the purpose of this study is to study the contact pressure on smooth follower and rough deformable cam surfaces in contact using finite element analysis (FEA). The plastic contact of a rough surface and smooth flat surface is analyzed by modeling the rough surface as an isotopic, Gaussian, and random process. For running FE analysis requires interface software to create a 3D model from the measurement data. The interface model was arranged by mathematical (MATLAB) and CAD (Solid work) software.

1.2 Statement of the problem

Most of the contact mechanisms are strongly linked to the pressure between the two surfaces in contact [9]. So far, different studies used numerical methods to investigate the effect of determining topography parameters on analyzing elastic contact between isotropic rough surfaces, numerical modeling of 3D rough surfaces to analyze interfacial contact characteristics and the contact behavior such as the pressure distribution, contact width, real area of contact and contact resistance of real rough surfaces. Various studies also tried to examine contact stress distribution on the cam profile,

the effect of surface finish and surface coating on the maximum subsurface stress, and the impact of surface finish.

However, different studies around the ignored the material property effects and the contacting body stress analysis in terms of contact pressure distribution and von mises stress has not yet been clarified. The effects of material properties with different density and surface finish on Moly based low alloy cam component subjected to contact load have not been studied numerically yet. Therefore, in this study two values of density of cam lobes, 7.35 g/cm^3 (Fe-1.5Mo- 0.3C) and 7.55 g/cm^3 (Fe-1.5Mo-0.2C) used as a variable property of the material with same surface finish property. Therefore, in this study a numerical method based on the finite element method by using ABAQUS software simulation to predict the contact pressure caused by the interaction between surfaces.

The expensiveness of the experimental method and the lack of sufficient study on cam subjected to contact load is the motive for this study. Therefore, this study aims to investigate the effect of surface finish and material properties on the carburized Moly based low alloy cam subjected to contact pressure at the critical point by using the numerical method utilizing ABAQUS software.

1.3 Objective of the Study

1.3.1 General Objectives

The general objective of this study is to investigate the effect of surface finish and material properties on the carburized Moly based low alloy cam subjected to contact load using the numerical method.

1.3.2 Specific objectives

- To determine the effect of material density variation on contact parameters
- To determine the effect of surface finish on contact parameters.
- To determine the effect of young's modulus

1.4 Scope and Limitation of the Study

This thesis will intend to probe the effect of surface treatment on the resistance of cam subject to contact pressure with the main objectives of modelling of the cam and follower contact mechanics, predicting the contact pressure at critical locations where the resistance of the cam is maximum associated with the process using numerical method using ABAQUS. The study also intends on two surface finish variations which are PM and machined surface. Furthermore, the study used two density

variations. Finally, this study has not included the study of wear and fracture analysis of the study do not investigate the analytical analysis and experimental study of the problem.

1.5 Significance of the Study

This study aims to model the contact pressure between contacting bodies to determine the effect of material density variation, surface finish, and young's modulus on contact parameters, and for a cam and follower arrangement using FEM. the study will show the effect of the parameters using an appropriate numerical method. Specifically, this study shows a new interface model to make a 3D finite element of the surface based on the measurement data that can be used for analyzing contact mechanics in the area of tribology. The methods are expected to assist researchers in material science, mechanical engineering, and particularly on better understanding the microscale surface contact mechanics. Furthermore, the result of problem gives a powerful potential for the manufacturing industries and academicians who want to study the tribological aspects of surface treatment process.

1.6 Organization of the Thesis

The study organized as of five chapters:

Chapter One: Presented the background of the topic about the contact mechanics, surface finish, mechanism of modeling surface finish, and the motive to do this study. Then, the statement of the problem formulates the existing problem related to the topic; the general objective and two specific objectives states the aims of the study to be achieved; scope and limitation of the study insights the scope and delimitation related to the study; and significance of the study presents the importance of the study.

Chapter Two: It discusses the theoretical and conceptual literature related to; surface finish, contact mechanics, surface roughness, contact problems on roughness, characteristics of random rough surface, numerical modeling of rough surface, and modeling techniques suitable for elastic contact. Furthermore, the empirical literature review gives a concise review of previous related studies to the topic.

Chapter Three: In this section, material selection and data collection; rough surface modeling; Modeling details of finite element formulation; and computational modelling of the problem wih the mesh independent test presented.

Chapter Four: In this chapter, the simulation results presented and discussed concerning different models under different parameters. Result of the effect of surface finish method on contact surface

and result of material density variation on contact parameters were discussed in detail with the help of graphs of the simulation results.

Chapter Five: Finally, conclusions are presented based on the result of the study and possible courses of action for the foundry and research areas point out for future recommendations.

Chapter 2: Literature Review

2.1 Theoretical and Conceptual Review

2.1.1 Surface finish

Surface finish is simply the condition in find the surface of the part at any point during the manufacturing process. This could be a primary finish, such as get from a pair of rollers in the rolling mill. Alternatively, it could be the finish get after aluminum is extrude through the die, or the finish on a sand casting before any post-processing. Next, there are secondary surface finishes created during CVC milling, turning, grinding, sanding, lapping or polishing. Each of these processes will impart its own characteristics finish to the surface. Then there are the many flavors of tertiary finishes produces by other treatments. Examples chemical passivation techniques like anodizing or galvanizing, electroplating with chrome or nickel, or decorative surface coatings such as painting or powder coating[10].

In general usage, the term surface finish is pretty much interchangeable with surface texture or surface topology. Topology literally means the way in which something is arranged, so in this case it means the way in which material is arranged on the surface of a part. Surface roughness is a bit different. This is quantifiable using a numerical unit called Ra. It's derived from measurements made of the surface profile using one of several different techniques and types of instruments. Some of these are contact type, using a very sensitive probe or stylus. Others are non-contact, using optical light, lasers, or even X-rays[10].

Surface finish, also known a surface texture or surface topography, is the nature of surfaces as defined by the characteristics such as lay, surface roughness, and waviness. Every part's surface is made up of texture and roughness which varies due to manufacturing techniques or processes.

2.1.2 Definitions and working mechanism of cam

A cam is a mechanical component of the camshaft and follower system that forces the follower (tappet) to move by direct contact. The cam's surface contour (profile) determines the motion of the follower. The cam is the driver (it runs at a constant speed), while the follower is the driven element. The cam can be stationary, translate, oscillate, or rotate, whereas the follower can be stationary, translate, oscillate, or index [11] .

Almost all mechanical devices and machines use cam-follower mechanisms (i.e., agriculture, transportation equipment, textiles, sewing machines, packaging, machine tools, printing presses, automobile internal combustion engines, food processing machines, switches, ejection molds, and control systems, and more recently in micromachines such as MEMS. In any class of machinery in which automatic control and accurate timing are paramount, the cam is an indispensable part of the mechanism. The possible applications of cams are unlimited, and their shapes occur in a great variety [17]. . An example of an engine cam and follower combination is shown in Figure 2.1.

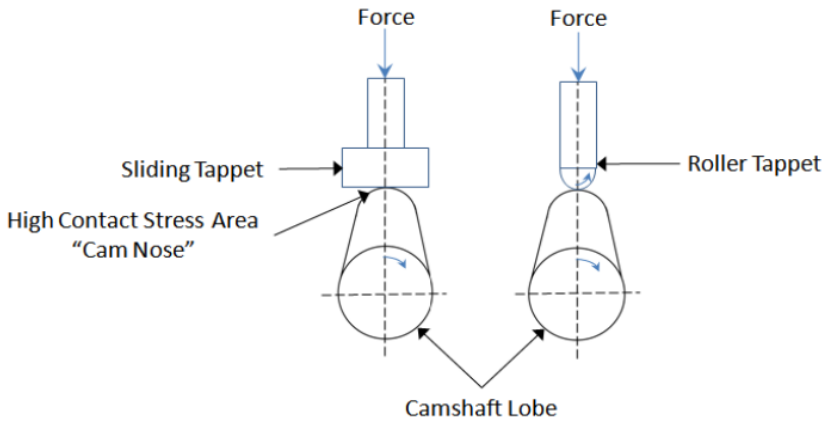

Figure 2.1: Cam and Follower system

The contact between the roller and the cam is a combination of sliding and rolling, resulting in a variety of failures. The contact's uniqueness is due to differences in a variety of characteristics such as radius of curvature, load, sliding velocity, and contact pressure angle all around the cam.

The pressure between the two surfaces in contact is strongly linked to the majority of wear mechanisms. For example, the Archard Law[12], the most common model of wear, is based on pressure and sliding velocity between the mating surfaces. In a first approach, it's common to assume that bodies in contact are topographically smooth. Nevertheless, the contact between solids is discontinuous in a realistic sense, and the real area of contact is a small percentage of the nominal area of contact. This is due to the topography of both surfaces, which only come into contact on a few places (asperities). At the interface of rough surfaces, the actual contact is between the asperities on the surface[13] As a result of the contact being concentrated on a small percentage of the nominal area, the microscopic pressures generated up are higher (Figure 2.2). Therefore, roughness has a strong impact on wear by means of real pressures of contact.

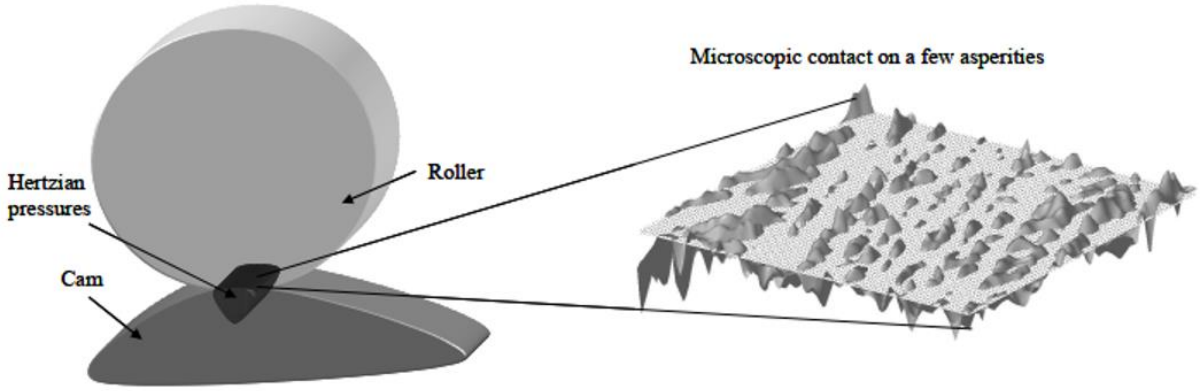

Figure 2.2: Nominal contact (left): distributed pressures. Microscopic contact (right): concentrated contact spots and higher pressure [13]

The mechanical and surface properties are essential for the characterization of materials. The requirement of products with good quality in terms of high strength, good surface finish, lower cost and less environmental effects is the challenge of the manufacturing industries [6]. Surfaces quality is one of the most specified customer requirements for machine parts. The major indication of surfaces quality on machined parts is surface roughness. The roughness of surfaces is considered as an essential parameter in many industries because it is an indication of the surface quality of the machined parts[16,17].

Because the final machining process is determined by surface roughness, the machining process in component manufacturing will affect the surface quality. As a result, different machining processes produce variable surface roughness [16]. Surface roughness is one of the most important requirements in machining process, as it is considered an index of product quality. It measures the finer irregularities of the surface texture. Achieving the desired surface quality is critical for the functional behavior of a part. Surface roughness influences the performance of mechanical parts and their production costs because it affects factors, such as friction, ease of holding lubricant, electrical and thermal conductivity, geometric tolerances and more. The ability of a manufacturing operation to produce a desired surface roughness depends on various parameters. The factors that influence surface roughness are machining parameters, tool and work piece material properties and cutting conditions[14].

For more than four decades, the impact of surface roughness pattern on the tribological performance of mechanical elements has been a touchy subject. Understanding the tribological performance requires knowledge of surface layer parameters. Bearings, gearboxes, camshafts, crank shafts, and other machine components require excellent tribological properties and practices to ensure longer life.

Many scientific problems involving friction, contact mechanics, heat conduction, electric current conduction, and component design require a thorough understanding of manufactured surfaces[17]. The surface finish of cam is important, because low roughness reduces friction and wear in the cam-roller contact[18].

2.1.2.1 Force analysis

The contact load acting on the cam-follower contact area changes depending on the cam rotation angle in the cam mechanism. At cam angles when the cam nose is in contact with the follower, the maximum contact load occurs[19].

Figure 2.3 shows the loading state of the smooth flat surface follower-roughness cam pair. Due to the flatness of the follower surface, the contact load is in the same direction as the centerline during a cam period. Only along the base circle does the contact load at the contact surface remain constant. With the cam pressure angle varying according to the cam rotation angle, the cam surface acts on the follower surface. As illustrated in Figure 2.3, the maximum value of the pressure angle occurs in the cam position, where the contact point of the two surfaces is furthest from center line. As a result, at the rotation angles corresponding to these positions, the cam stays under the effect of the maximum torque [19].

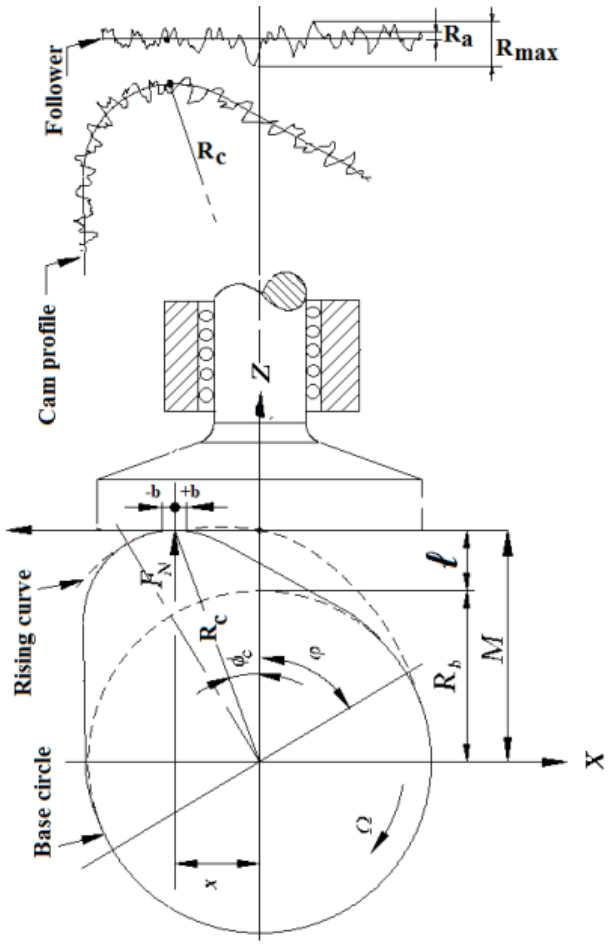

Figure 2.3: Roughness consideration in a cam and flat surfaced follower pair[19]

2.1.3 Contact Mechanics

2.1.3.1 Introduction

Contact phenomena abound in everyday life, and thus play a critical role in the design of structures and systems. They include, friction, wear, adhesion, and lubrication, among other things; are inherently complicated and time-dependent; occur on the outer surfaces of parts and components, and involve thermal, physical, and chemical processes; and are inherently complex and time-dependent. The study of relative motion, interacting forces, and tribological behavior of two rigid or deformable solid things that touch or rub on each other along sections of their borders throughout time intervals is known as contact mechanics. The interaction of deformable bodies, on the other hand, is extremely complex and little understood.

Historically, there have been two techniques to study the contact behavior of deformable bodies. The first assumes that the bodies are smooth and that their nominal geometry can sufficiently characterize

them, whereas the second admits that all surfaces have a multitude of peaks and valleys that have a significant impact on the nature of the contact.

2.1.3.2 Hertzman contact

Hertz produced the first significant elastic contact analysis of surfaces[20].The benchmark work of Hertz (1882) considered the contact between normally loaded nonconforming bodies, which are homogenous in microstructure (material), frictionless surface and undergoes only elastic deformation, to analyze surface deformation shape and contact stress distributions[21]. The Hertz model only analyzes the elastic contact and excludes the effects of roughness and plasticity, as well as the real contact area. The Hertzian formulation of contact between cylinders, which can be equated to a cylinder-on-elastic-half-space equivalent, is used to calculate the stress state of a pure material at a specific depth and location.

Hertzian contact assumptions:

- Stress and displacement must satisfy the differential equation of equilibrium foe each elastic body and stresses vanish at great distance from the contact zone.
- The contact body are in frictionless contact, that is only normal pressure is transmitted between the two contacting bodies.
- The profile of the opposing smooth surfaces is represented by quadratic function. The distance between the two surfaces are zero inside and greater than zero outside the contact area.
- At the surface of bodies, the pressure is equal and opposite inside the contact area and zero outside. The integral of pressure distribution within the contact area balance the normal force acting between the two bodies.
- The pressure distribution on the contact area is ellipsoidal.
- A quasi-static analysis is considered. Because of very low deformation and strain of the slave disc
- The width of the contact is small compared to the body radii.

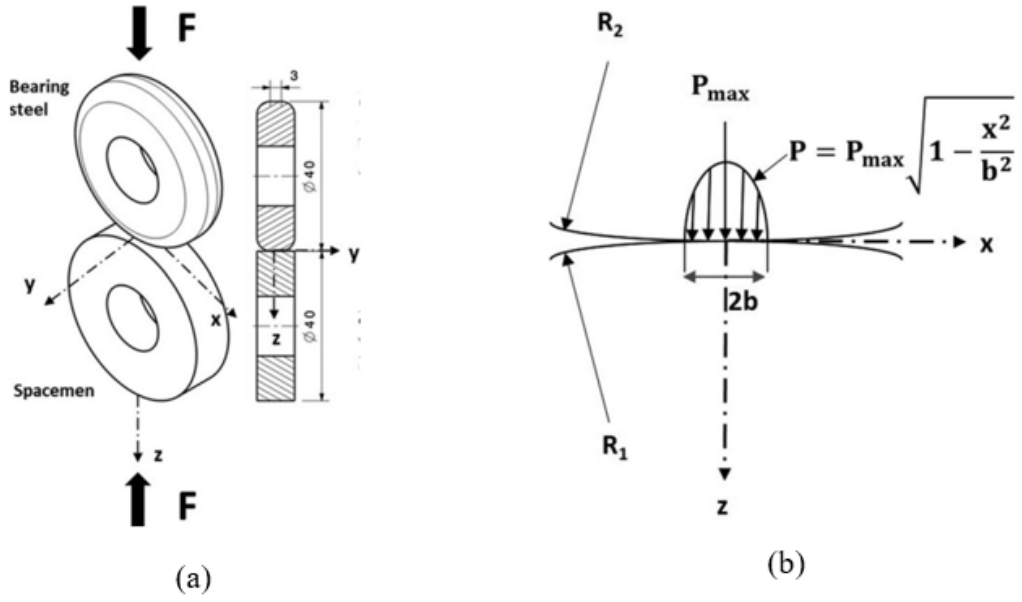

Figure 2.4: Contact between cylindrical surfaces (a) and parabolic pressure distribution (b) [22]

According to the Hertzian contact theory, the pressure distribution (P) is parabolic in shape in the contact width (2b); pressure becomes maximum $\left(P_{\max}\right)$ at the middle of the contact zone. The 2-D Hertzian stress distribution on x-z plane determines using formulas eq. 2.1 to eq. 2.5

$$\sigma_x = \frac{P_{\max}}{b}\left\{m\left(1+\frac{z^2+n^2}{m^2+n^2}\right)-2z\right\} \qquad 2.1$$

$$\sigma_z = \frac{P_{\max}}{b}m\left(1-\frac{z^2+n^2}{m^2+n^2}\right) \qquad 2.2$$

$$\sigma_y = \nu\left(\sigma_x+\sigma_z\right) \qquad 2.3$$

$$\tau_{\max} = \begin{Bmatrix} \tau_{xz} = \dfrac{\sigma_z-\sigma_x}{2}, \dfrac{z}{b} < 0.463 \\ \tau_{yz} = \dfrac{\sigma_z-\sigma_y}{2}, \dfrac{z}{b} > 0.463 \end{Bmatrix} \qquad 2.4$$

$$\sigma_{eq} = \frac{1}{2}\left[\left(\sigma_z-\sigma_x\right)^2+\left(\sigma_y-\sigma_x\right)^2+\left(\sigma_z-\sigma_y\right)^2\right]^{0.5} \qquad 2.5$$

Where, m and n are variables described in terms of space X, Z coordinate and determined in equation 2.6 and equation 2.7

$$m^2 = \frac{1}{2}\left[\left\{\left(b^2 - x^2 + z^2\right)^2 + 4x^2z^2\right\}^{\frac{1}{2}} + \left(b^2 - x^2 + z^2\right)\right] \quad 2.6$$

$$n^2 = \frac{1}{2}\left[\left\{\left(b^2 - x^2 + z^2\right)^2 + 4x^2z^2\right\}^{\frac{1}{2}} - \left(b^2 - x^2 + z^2\right)\right] \quad 2.7$$

The sign of m and n are associated with the sign of z and x axis, respectively.

The mean Hertzian pressure (Po) applied on the cylindrical contact surface is determined using the relation given by eq. (2.8).

$$P_0 = 0.78P_{\max} \quad 2.8$$

Where maximum pressure is given by eq. (2.9)

$$P_{\max} = \frac{2F}{\pi bL} \quad 2.9$$

Half contact width b relates to the effective elastic modulus (Ec), the effective radius (Rc) of curvature, and the applied load (F) and is determined using eq. (2.10).

$$b = \sqrt{\frac{4R_cF}{\pi LE_c}} \quad 2.10$$

Where Ec and Rc are evaluated using eq. (2.11) and eq. (2.12), respectively

$$\frac{1}{R_c} = \frac{1}{R_1} + \frac{1}{R_2} \quad 2.11$$

$$\frac{1}{E_c} = \frac{1-\nu_1^{\,2}}{E_1} + \frac{1-\nu_2^{\,2}}{E_2} \quad 2.12$$

Here, E_1 and E_2 are the moduli of elasticity and ν_1 and ν_2 the Poisson's ratios of both bodies.

2.1.3.3 Non-Hertzian elastic contact

Violations of the Hertzian assumptions

- The surfaces separation cannot be expressed as a quadratic form
- The common generatrix has a finite length
- The contacting surfaces are no longer smooth
- The presence of friction

Finite element method

- It needs very fine mesh for contact study
- It needs a lot of time and cost
- Is not very common to study contact

Analytical formulation for Non-Hertzian contact elastic contact: the shape and size of the real contact area as well as the pressure distribution on it are unknown.

2.1.3.4 Contact of nominally flat rough surface

Though cam has a curved surface for the modeling of the contact between the cam and follower assumed to be flat in different studies since modeling the curved surface on MATLAB is difficult, and the size of the contact area for the modeling is small [13]. On a microscopic scale, all surfaces are rough, and when two rough surfaces come into contact, the real area of the contact is very small compared to the apparent area of the contact.

Only some peaks of two rough surfaces will be in contact when loading presses, them together, hence these peaks often carry very high loads. Greenwood and Williamson investigated this effect in 1966 [23].

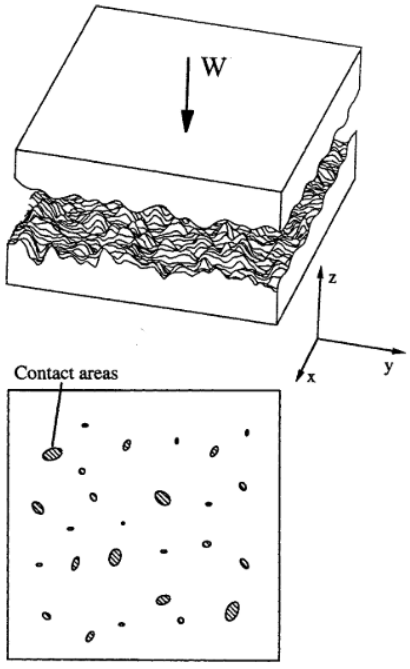

Figure 2.5: Schematic of the real area of contact[24]

One of the earliest models of elastic asperity contact is Greenwood and Williamson's [23] . This is a statistical model based on the following assumptions:

- The rough surface is covered with a large number of asperities, some of, which, are spherical, at least near their pea;
- On each surface, the radius of asperity summits is constant;
- Height of asperity varies at random;
- Peak heights on most engineering surfaces have a Gaussian distribution.

A contact between one smooth surface and one rough surface can be used to simplify the analysis of a contact between two rough surfaces. The rough surface has an equivalent roughness of the two surfaces. The asperity curvature of this equivalent rough surface is equal to the sum of the curvatures of the two rough surfaces:

$$\frac{1}{R_p} = \frac{1}{R_{p1}} + \frac{1}{R_{p2}} \qquad 2.13$$

and the standard deviation of the equivalent rough surface is given by:

$$\sigma_p = \sqrt{\sigma^2{}_{p1} + \sigma^2{}_{p2}} \qquad 2.14$$

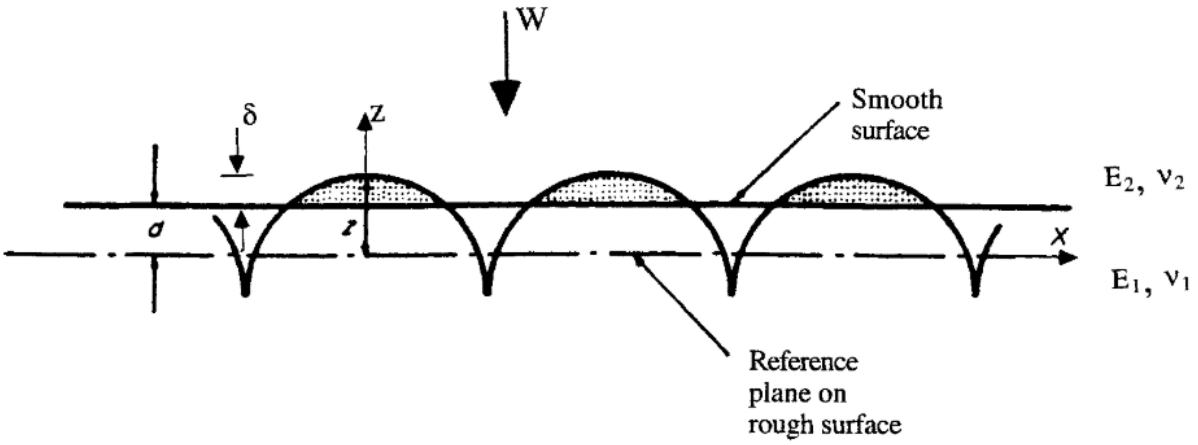

Figure 2.6; Schematic of the contact between rough surface against a smooth plane surface [24]

The Hertzian equations describe the behavior of a single asperity, load W_i and the area of contact A_i for each asperity is:

$$W_i = \frac{4E^*}{3} R^{1/2} \delta^{3/2} \qquad 2.15$$

and

$$A_i = \pi R \delta \qquad 2.16$$

For N asperities the total load W_t will be equal to NW_i, and the total area

$$A_t = NA_i = N\pi R\delta \qquad 2.17$$

then:

$$W_t = NW_i = N\frac{4E^*}{3}R^{1/2}\delta^{3/2} \qquad 2.18$$

$$W_t = N\frac{4E^*}{3}R^{1/2}\left(\frac{A_t}{N\pi R}\right)^{3/2}, \delta = \frac{A_t}{N\pi R}$$

$$W_i = \frac{4E^* A_t^{3/2}}{3\pi^{1/2}N^{1/2}R} \qquad 2.19$$

The critical load beyond which the plastic deformation occurs can be estimated calculating the mean (pm) or maximum contact pressure (p0):

$$p_m = \frac{2}{3}p_0 = \frac{W_i}{A_i} = \frac{4E^*\delta^{1/2}}{3\pi R^{1/2}} = \left(\frac{16WE^*}{9\pi NR^2}\right)^{1/3} \qquad 2.20$$

Using the Von Mises shear stress energy criterion, the initial yielding is initiated for: $p_m \approx 0.9Y \approx H/3$, then the critical load which the plasticity occurs is:

$$\frac{W_{crit}}{N} \approx \frac{\pi^3 R^2 H^3}{48E^{*2}} \qquad 2.21$$

or a contact between one rough surface and a smooth plane, Greenwood and Williamson proposed to analyze this contact with amplitude distribution function:

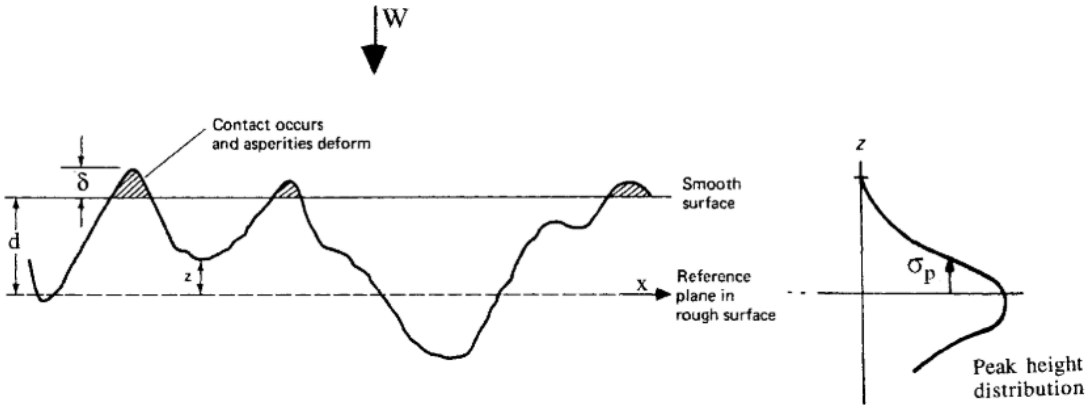

Figure 2.7; Schematic representation of the contact between a rough surface and a smooth surface, and representation of the amplitude distribution function [24].

If the two surfaces are separated by a distance d, the probability of making contact at any given asperity of height z is:

$$P(z > d) = \int_d^\infty \phi(z)dz \qquad 2.22$$

and if there are N asperities in the surface, the probability of the number of contacts is:

$$n = N\int_d^\infty \phi(z)dz \qquad 2.23$$

also, $\delta = z - d$ and $A_i = \pi\delta R_p$ the expected contact area of the contact will be given by:

$$A_i = \pi N R_P \int_d^\infty (z-d)\, p(z)dz \qquad 2.24$$

and the total load is:

$$W_t = p_t A_t = p_n A_n = \frac{4}{3} N E^* R_P^{1/2} \int_d^\infty (z-d)\, p(z)dz \qquad 2.25$$

Using standardized variables, and describe heights in terms of the standard deviation σ of the height distribution. Also, introducing the surface of asperity summits per unit area: $N = \eta A_n$, where η is the density of asperities, gives:

Number of contact spots:

$$n = \eta A_n F_0(D) \qquad 2.26$$

Total contact area:

$$A_t = \pi\eta A_n R_p \sigma_p F_1(D) \qquad 2.27$$

Load:

$$W = \frac{4}{3}\eta A_A E^* R_p^{1/2} \sigma_p^{3/2} F_{3/2}(D) \qquad 2.28$$

Where D is the dimensionless separation: $D = d/\sigma_P$ and $F_m(D)$ is a parabolic cylinder function and is given by:

$$F_m(D) = \int_D^\infty (s-D)^m p^*(s)\, ds \qquad 2.29$$

for the case that the amplitude distribution function is a Gaussian distribution:

$$p^*(s) = \frac{1}{(2\pi)^{1/2}} \exp\left(-\frac{s^2}{2}\right) \qquad 2.30$$

$$F_m = \left[\frac{1}{(2\pi)^{1/2}}\right] \int_D^\infty (s-D) \exp\left(-\frac{s^2}{2}\right) ds = \left[\frac{m!}{(2\pi)^{1/2}}\right] \left[\exp\left(-\frac{D^2}{4}\right)\right] U\left(m+\frac{1}{2}D\right) \text{ for the case } m \geq 0$$

2.1.4 Surface Roughness

Depending on the nature of the solids, the method of surface preparation, and the interaction between the surface and the environment, a solid surface, or more precisely a solid–gas or solid–liquid interface, has a complicated structure and complex properties. Although surface parameters affect real area of contact, friction, wear, and lubrication, solid surface properties are critical to surface interaction. Surface qualities are essential in various applications besides tribology, including as optical, electrical, and thermal performance, painting, and appearance[25].

2.1.5 Contact Problem on Rough Surfaces

Surfaces were historically modeled analytically using assumptions and simplifications. Any typical machining/manufacturing method can never generate a smooth surface. Asperities are the irregularities on the surface. A number of geometric shapes were used to model asperities. Numerous writers have used analytical methods to investigate the problem of rough surface contact in the past (Whitehouse & Archard [26]; Onions & Archard [27]; Bush, Gibson, et al, [28]; Hisakado, T. [29]). Their outcome was quite useful; however, it can only be used for a restricted range of loads.

The height of the asperity on the surface and the pattern of contact were treated as probability distributions. Extrapolating the behavior of a single pair of interacting asperities to a pair of interacting surfaces covered with asperities was common [30]. The contact itself is typically investigated using either a stochastically or deterministically based technique. Greenwood and Williamson [31] proposed one of the first models, assuming that the asperity summits are spherical with a constant radius, that the asperities deform elastically, and that their height follows a Gaussian distribution. Statistical models have had a significant impact on contact analysis, and many authors [32 ,36–38] have considered using it. However, these models ignore real geometry of the surface and the interactions between the asperities. To introduce a more precise geometric description, deterministic approaches were developed [34].

In recent years, researchers have worked on real-surface analysis either experimentally [35] or using FE software to develop a rough surface model. Contact simulation with complicated geometry, boundary conditions, material properties, and material models is feasible with FE modeling.

2.1.6 Characteristics of random rough surfaces

Surface topographies are inherently complex due to the statistical character of many surface finishing procedures such as polishing and grinding. Average roughness parameters, statistical roughness parameters, random process parameters, and fractal roughness parameters are also the types of roughness parameters. The Centre line average (CLA, Ra) and the root mean square (RMS, Rq) are the two most commonly utilized roughness parameters. Statistical descriptors are needed to characterize such surfaces. Descriptors, such as root mean square (rms) roughness, which attempt to quantify some feature of surface statistics with a single number, and surface statistical functions, such as power spectral density, are the two types of descriptors [6, 15].

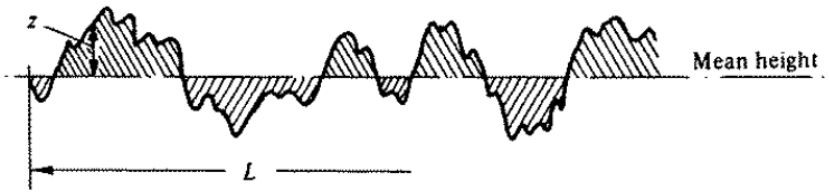

Figure 2.8 Profilometer trace [24]

The average roughness is now defined by

$$R_a = \frac{1}{L}\int_0^L |z| dx \qquad 2.31$$

Where, $z(x)$ is the height of the surface above the datum and L is the sampling length. The root mean square or standard deviation of the height of the surface from the Centre-line is a less common but statistically more important measure of average roughness., i.e.

$$\sigma^2 = \frac{1}{L}\int_0^L z^2 dz \qquad 2.32$$

The nature of the surface influences the relationship between σ and R_a to some extent [36]

- For a regular sinusoidal profile;

$$\sigma = \left(\pi / 2\sqrt{2}\right) R_a \qquad 2.33$$

- For a Gaussian random profile;

$$\sigma = (\pi/2)^{1/2} R_a \qquad 2.34$$

2.1.7 Numerical modeling of rough surfaces

2.1.7.1 Introduction

Surface texture is the three-dimensional topography of a surface that is formed by repetitive or random deviations from the nominal surface. Roughness (Nano and microroughness), waviness (macroroughness), lay, and flaws are all forms of surface texture. The textures of most engineering surfaces are random, either isotropic or anisotropic, and either Gaussian or non-Gaussian. Whether the surface height distribution is isotropic or anisotropic and Gaussian or non-Gaussian depends upon the nature of the processing method [25].

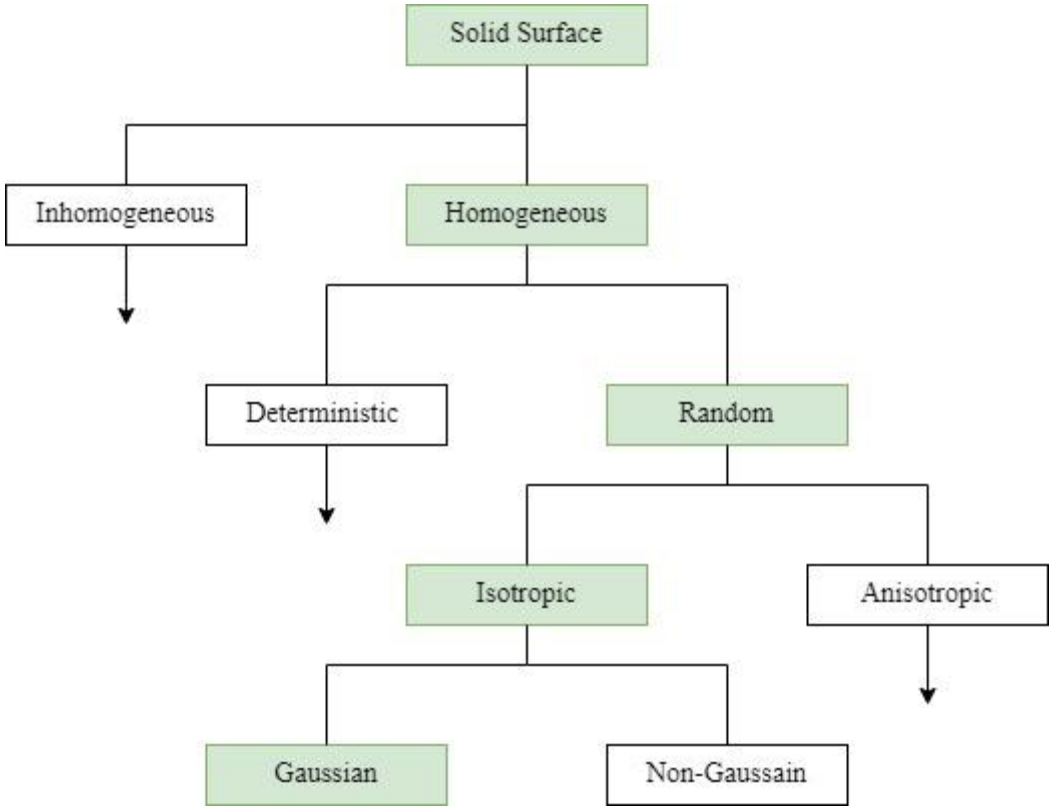

Figure 2.9: General typology surfaces

Modeling the rough surface as an isotopic, Gaussian, random process is used to investigate the elastic contact between a rough surface and a smooth flat surface [37].

2.1.7.2 Statistical characteristics

On the micro-scale, the real surface topographies of rough interfaces are so irregular that they can only be well described by statistical characteristics, the parameters of which are calculated using the

height distribution, probability density function (PDF), power spectral density (PSD), or autocorrelation function (ACF) [38].

2.1.7.2.1 Probability density function (Gaussian height distribution)

The Gaussian distribution, often known as the normal distribution, is probably the most significant distribution in all of statistics. A Gaussian distribution (sometimes called the natural or normal distribution), is probably the most significant distribution in all of statistics. The Gaussian distribution is used to model continuous random variables in a variety of situations. The central limit theorem states that in the limit, the average of a large number of independent identically distributed random variables approaches the normal distribution, which is why the Gaussian distribution is so important [9, 10]. The normal probability function is useful in the analysis of randomly rough surfaces from a mathematical perspective. The Gaussian distribution has a variety of interesting properties. It can be shown that

- The sum of independent Gaussian random variables is Gaussian.
- Random variables are jointly Gaussian if an arbitrary linear combination is Gaussian.
- Uncorrelated jointly Gaussian random variables are independent

The probability density function of a single gaussian random variable is denoted as $N(\mu,\sigma)$ and defined as:

$$f(x)=\frac{1}{\sqrt{2\pi\sigma^2}}\exp^{-\left(\frac{1}{2\sigma^2}(x-\mu)^2\right)} \qquad 2.35$$

The Gaussian is described by two parameters:

- The mean μ (location)
- The variance σ^2 (dispersion)

Where, σ the width of the Gaussian or is the standard deviation. The exponential function, $-\frac{1}{2\sigma^2}(x-\mu)^2$, is a quadratic function of the variable x. Furthermore, the parabola points downwards since the quadratic term is negative. The factor $\frac{1}{\sqrt{2\pi\sigma^2}}$, is a constant that is independent of x; as a result, we can think of it as a "normalization factor" of the distribution so that

$$\frac{1}{\sqrt{2\pi\sigma^2}}\int_{\infty}^{\infty}\exp-\left(\frac{1}{2\sigma^2}(x-\mu)^2\right)=1 \qquad 2.36$$

i.e. The area under the curve, or total probability, is one.

All Gaussians have the same shape, with the location controlled by the mean, and the dispersion (horizontal scaling) controlled by the variance. Figure 2.3 shows a one-dimensional Gaussian with zero mean and unit variance (μ=0, σ2 =1.) The mean and variance of a Gaussian distribution determine its shape. When a Gaussian random variable has a zero mean and unity variance, it is referred to as a standard Gaussian random variable $N(0,\sigma)$.

$$f(x)=\frac{1}{\sqrt{2\pi\sigma^2}}e^{-\left[\frac{x^2}{2\sigma^2}\right]} \qquad 2.37$$

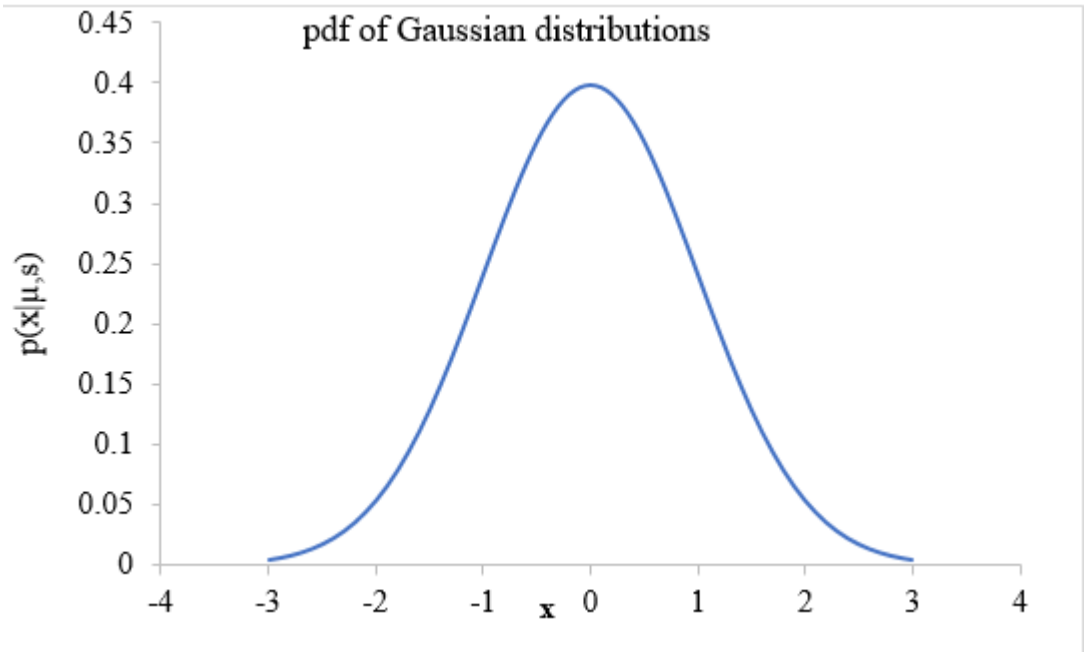

Figure 2.10: One dimensional Gaussian (μ=0, σ2=1)

The behavior of the pdf with respect to the variance parameter is shown in Figure 2.11 .

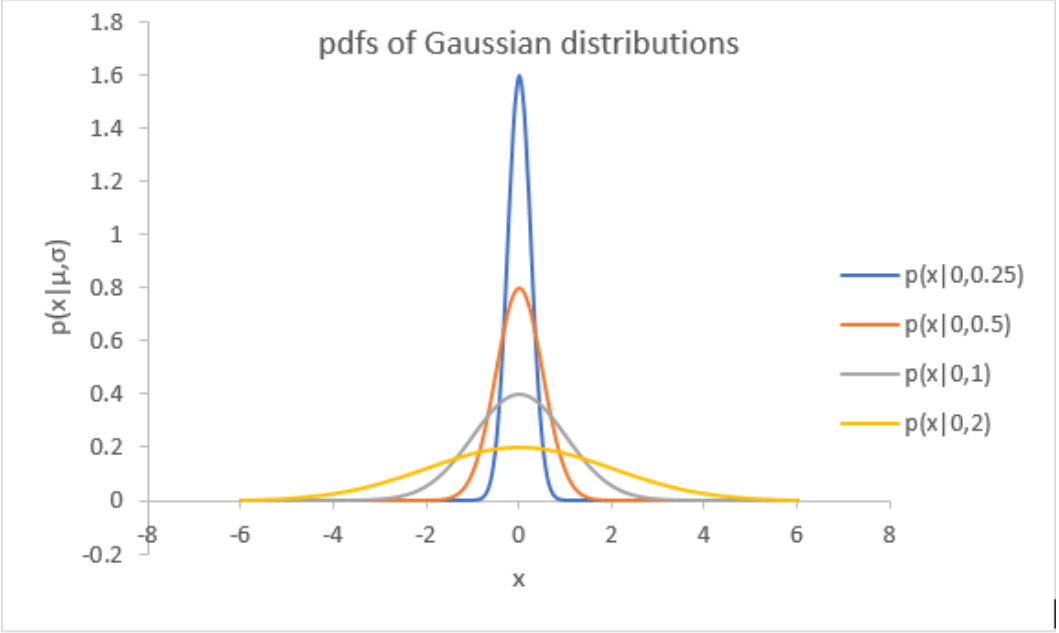

Figure 2.11: Four Gaussian pdfs with zero mean and standard deviation

2.1.7.2.2 The autocorrelation function and the power spectral

The autocorrelation function reflects the relationship between the amplitude of the surface heights and the wavelength, and describes the dependence of peak values at one point on height values at another position [41]. Within the discrete shape, the autocorrelation function of surface is characterized as

$$R = E\left[x(t_1), x(t_2)\right] = \int_{-\infty}^{\infty}\int_{-\infty}^{\infty} x_1 x_2 p_x(x_1, t_1, x_2, t_2)\, dx_1 dx_2 \qquad 2.38$$

For the characterization of a random Gaussian process, these two moments may be adequate. The ensemble average E[.] must be determined, as stated in the previous formulae. Instead of specifying the value for a set of samples at a given time, it is more convenient to consider only one sample and calculate the average varying time, according to the Ergodicity theorem [42]. On a single sample, the autocorrelation function of a stationary process is

$$R(\Delta t) = \lim_{T\to\infty} \int_{-T/2}^{T/2} x(t)x(t+\Delta t)\, dt \qquad 2.39$$

This function has some essential qualities; for instance, the autocorrelation function's value at the origin is equal to the sample's variance:

$$R(\Delta t)=\lim_{T\to\infty}\int_{-T/2}^{T/2}\left[x(t)\right]^2 dt=\sigma^2 \qquad 2.40$$

Because the autocorrelation function is nonnegative, the Fourier transform of this function is also positive, and the power spectral density (PSD) is the Fourier transform of R.

$$s_{xx}(\omega)=\frac{1}{2\pi}\int_{-\infty}^{+\infty}R(\tau)e^{j\omega\tau}d\tau \qquad 2.41$$

If $s_{\eta\eta}$ denotes the PSD of input sequence, the relation $s_{\eta\eta}$ and s_{xx} for a linear system have the form

$$s_{xx}(u,v)=\left[H(u,v)\right]^2 s_{\eta\eta}(u,v) \qquad 2.42$$

where $H(u,v)$; is the frequency response or transfer function of the system.

Since $f(x,y)$ is a sequence composed of independent random number, its spectral density is a constant $(s_{\eta\eta})$

$$s_{\eta\eta}(u,v)=constant=c \qquad 2.43$$

It is reasonable to create a filter with a real frequency response and filter coefficients satisfying for the generation of random surfaces.

$$h(x,y)=h(-x,y)=h(-x,-y)=h(x,-y) \qquad 2.44$$

According to this discussion, the transfer function could be obtained from

$$H(u,v)=\sqrt{\frac{s_{xx}(u,v)}{c}} \qquad 2.45$$

Where, $H(u,v)$ is the Fourier transform of $h(x,y)$ and $s_{\eta\eta}$ is the power spectral density of input sequence. If the input power spectral density is given by a Gaussian white noise with a mean zero and magnitude 1($s_{\eta\eta}(u,v)=1$)[43], then

$$s_{xx}(u,v)=\left[H(u,v)\right]^2 \qquad 2.46$$

$$H(u,v)=\sqrt{s_{xx}(u,v)}, \qquad 2.47$$

The well-known Fourier transform is used to relate the time and frequency domains shown in the Figure 2.12.

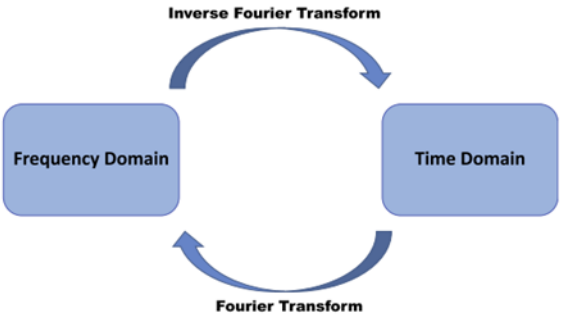

Figure 2.12: Time-frequency relationship

2.1.7.3 Mathematical rough surface model

The rough surface in this study was generated using mathematical software and was based on a mathematical equation. To create a surface with random roughness, Gaussian equations were utilized. Two parameters can be used to describe a surface with a gaussian height distribution and an exponential autocorrelation function: the standard deviation of surface heights (σ or Rq or rms) and the correlation length (β∗). Peak-to-mean distance (Rp) and peak-to-valley (P–V) distance are two more often studied characteristics. Because of the multiscale nature of surfaces, the surface roughness characteristics are found to be highly dependent on the measuring instrument's resolution or any other type of filter, and so are not unique for any given surface[24].

2.1.7.4 Generation of random surface

The height at any point on the surface is the random variable. An infinite number of random values derived up a random process. As a result, roughness can be considered of as a random process. The common statistic parameters used in static contact analysis are defined in this section.

The statistical considerations shows the majority of today's surface geometry parameters are essentially estimates of the height distribution, autocorrelation, or a combination of the two [44]. The height distribution and the autocorrelation function are two statistical functions that characterize rough surfaces as a random process (ACF). The surface amplitude discrete samples correspond to a 2-D random sequence. To imitate real rough surfaces, random sequences with a particular type of height distribution and ACF must be generated.

The input sequences f(x, y) comprising of independent random numbers are first generated using random number generators. The random surface output sequences g(x, y) are then obtained through the filtering procedure, which gives the sequences a specific form of the ACF. When the sequences pass through the linear system, the distribution of the input sequences remains unchanged [45].

2.1.8 Modelling techniques suitable for Elastic contact with Abaqus

2.1.8.1 Introduction

This section discusses how to use the Abaqus Finite Element (FE) program to study elastic contacts. For both the cam and the follower, a representative profile has been selected from the experimental work. This work to examine elastic contact analysis depends on the roughness profiles, which can also be taken from cam nose is in contact with the follower.

2.1.8.2 Numerical analysis of contact problems in Abaqus

In general, contact refers to the study of deformable bodies that come into contact with each other at least once during the simulation process, allowing contact stress to be transmitted between the two bodies when a load is applied. Contact problems are generally caused by a continuum contact with a large number of nodes in contact when under load. Such contact may cause local deformation and stress.

In Abaqus CAE software package, a contact problem requires: definition and creating of model parts that may be in contact, model meshing, definition of pairs of surfaces that interact (contact interactions), specifying property assignments of the surfaces in contact with each other, specifying contact properties including such tangential mechanical properties (friction) and Young's modulus [33].

2.1.8.3 Meshing element type and their effect

The "Complete Abaqus Environment," or "Abaqus CAE," provides a wide range of elements for various contact problems and analysis types. The number of nodes (which depends on the element shape and interpolation method), formulation (small- and finite-strain shells), degrees of freedom per node (which depends on the field variable), and integration method (reduced and full integration) are all characteristics of the Abaqus element. From an engineering perspective, not only does the element type influence the accuracy of the results, but the mesh size selection also has a significant impact on the Abaqus modeling structure. The mesh size has a significant impact on the accuracy of numerical simulation results, so choosing the best meshing approach when modeling a rough surface is essential [33].

Managing mesh characteristics

Changes in element sizes from region to region should be accommodated using a finite element mesh. A mesh must be conforming in order for Abaqus FEM packages to work. This means that nearby

components must share a whole edge or face. In terms of the accuracy of the analysis at the asperity level and the localized stresses in the surrounding material, the number of elements and mesh resolution at the surface are important. The geometry was initially separated into shapes that are more readily processed by the pre-processor tool in order to build a sufficient mesh and acquire a high resolution at and around the contact region for the rough r component that has strange geometric shapes. The meshing of the partitioned geometry part was controlled using an appropriate algorithm. To improve mesh quality, the mesh is controlled by using the partition tool sets. As a result, different mesh local densities might be implemented more efficiently in different edge of the model. A finer mesh was employed near the contact area between the rough portion and the smooth section. The transition between these various districts was kept smooth to avoid discontinuity in results at partition edges.

2.1.8.4 Penetration of master surface to slave surface in contact analysis

The interactions and constraint features applied to master and slave surfaces form the basis of Abaqus/general Standard's contact algorithm. For each contact pair, the user must designate a master and slave surface. It is also recommended that analytical rigid surfaces and rigid element-based surfaces be master surfaces at all times. The master rough part surface should be coarsely meshed, whereas the slave rough part surface should be finely meshed. One of two ways, node-to-surface discretization or surface-to-surface discretization, can be used to define the contact interaction and penetration definition between the surfaces. Each slave node interacts with a group of master surface nodes in the node-to-surface technique. As a result, the slave nodes are assumed to not penetrate the master surface, but the master surface nodes are assumed to penetrate the slave surface.

2.2 Empirical Review

Lee H. P. et al. [46] studied the contact mechanics of surfaces with various models of roughness descriptions to examine the differences in rough surface descriptions on the stress analysis of head-disk interface among various models. The study employed a mathematical expression to model the rough surface of the model employing polynomials and Fourier series to describe the surface height variation. The computational method employed FEM using ABAQUS to perform Elastic-plastic contact analyses for the head-disk interface (HDI). The result of the study depicted that, the maximum von Mises equivalent stress for carbon overcoat and the magnetic layer has a magnitude micro contacts, with the region from x = 130 to 160 nm of 3.86 GPa, less than the yield strength of the carbon overcoat, which occurs directly on top of the right asperity at decreases gradually from the two inner

contours to the outer. Furthermore, the numerical result showed that the maximum interference distance is up to 1 nm, and the deformation in the disk medium is elastic. Experimental Validation of the FEM method-using ABAQUS was not included in the study and contact body stress analysis (contact pressure and surface shear stress) were not studied.

Molinari J.F. [47] probes a FEM utilizing an explicit dynamic Lagrangian framework for the modeling of elastoplastic contact between rough surfaces to the model of elastoplastic contact between rough surfaces using frictionless, no adhesive, contact between a rigid plane and an elastoplastic solid with a self-affine fractal surface. The FEM used to establish a relationship between contact properties and key material parameters. The result of simulation depicted that, the contact area rises linearly with the applied load, the rate of increase grows as the yield stress σ_y decreases, scaling as a power of σ_y over the range typical of real materials. The result also showed that plasticity produces qualitative changes in the distributions of local pressures in the contact and the size of connected contact regions. Furthermore, result of the computational model reveals that, the total plastic work is found to be nearly constant over a wide range of yield stresses. In the study, the validation of the numerical results with the experimental method was not included and contact stress between the rigid contacting surfaces was not calculated.

Soejima and Nagafuji [48] studied the influence of cam surface finish and roughness on frictional power loss in valve trains with roller tappets to examine the impacts of surface finish and roughness of cam on frictional power loss in valve trains with roller tappets. the methodology used in the study was measuring the contact load (Fc) and the friction force (Ff) with a practically sized OHV typed valve train friction test rig. The result of the study showed that the influence of surface finish and roughness of the cam lobe on the friction loss in the valve train is quite small. Moreover, under the high rotation speed of the camshaft, the friction coefficient decreases as the surface roughness becomes large. The rough cam surface prevents skidding of the rolling contact because the bearing ratio of solid contact is large. The result also depicted that the surface roughness should be larger than one micron and smaller than around three microns root mean square. Furthermore, Shot-peening is more desirable than grinding as the finish of the cam lobe for a valve train with roller tappets. In the study, contact stress between the cam and follower and Contact pressure of the system was not studied.

Hua D. Y. et al. [49] studied multi-scale system analysis and verification for improved contact fatigue life cycle of a cam-roller system to analyze the Contact of cam and roller with rough surfaces to examine the effects of surface finish and surface coating on maximum subsurface stress. Micro-

contact analysis module of a Surface Distress Analytical Toolkit was used to Measure the subsurface stress of the cam and roller. The result of subsurface stress was confirmed by laboratory tests using six rollers with various degrees of finishing processes, and with and without the addition of coating to the surfaces. In addition, Smooth surface provides a 53% reduction in maximum subsurface stress and addition of coating further reduces subsurface stress by nearly 7%. The result also depicted that the impact of the combined treatment of the surface is an increase in contact fatigue life of the cam-roller system by nearly two orders of magnitude. The examination of the rollers in the laboratory indicates a general improvement in roller performance due to the addition of a coating. Furthermore, Combination of finishing process and coating was found to provide the best contact fatigue life since the corresponding rollers showed no observable wear even after testing for 2161 h, or the same number of cycles accumulated over about 500,000 truck miles. Finally, the result depicted that the nominal area of contact and the number of points that describe the surface were kept constant for all calculations. The study does not show the real contact area, and Pressure distribution over the cam and follower and effect of density variation of the material is not presented and analyzed.

Cailletaud G. [33] examines rough surface contact analysis using the Finite Element Method and a new reduced model to model a normal frictionless mechanical contact between an elastoplastic material and a rigid plane. Result of the study illustrated that the evolution of the contact force versus the displacement of the rigid foundation is non-linear, with a power of 3.4. Furthermore, on the force-displacement curve, for the maximum displacement, the simplified prediction made without interaction overestimates the force by 40%. The study predicts the load-displacement curve, real contact area, and the free volume only at single asperities.

Jiang Z. et al. [50] studied the surface roughness during metal manufacturing to analyze the surface roughness transfer during cold strip rolling using a numerical simulation using ABAQUS and experimental validation of the numerical result. The result of the computational and experimental study revealed that, surface roughness decreases significantly with an increase or reduction considering the friction effect. The study also showed that lubrication can delay surface asperity flattening and the surface roughness affects the crack initiation significantly in cold strip rolling. Furthermore, the surface roughness variation along the metal plate width contributes to stress distribution and then inhibition of crack nucleation. In the study contact, body stress analysis (contact pressure and surface shear stress) and contact body area was not studied.

Raeymaekers B. et al. [51] analyzed the effect of determining topography parameters on analyzing elastic contact between isotropic rough surfaces to study the elastic contact between two computer-generated isotropic rough surfaces. The methodology employed in the study was a numerical method to generate the isotropic 3D rough surfaces by using Gaussian distribution of asperity heights. The asperity density is obtained using the spectral moment's method and the summit identification method. The result of the study depicted that it was found to be significantly smaller for the summit identification method than for the average spectral moment. Furthermore, the effect of the autocorrelation on the resulting contact parameters obtained from the four different models was examined, and it was found that for increasing autocorrelation length, the resulting contact parameters become less sensitive to the sampling interval, irrespective of the method to determine the topography parameters. In this study, contact stress and contact pressure between the cam and follower was not studied.

Li B. et al. [38] analyzed the numerical Simulation of 3D rough surfaces and analysis of interfacial contact characteristics to analyze interfacial contact characteristics by applying numerical simulation using FEM. result of the study showed that the improvement of the surface quality and the increment of the assembly load can be beneficial to enhance the contact stiffness. The ratio of Ar/Ao of real contact presents a nonlinear increment with the rise of the normal displacement d while a nearly linear one with the rise of the nominal pressure P_0. Furthermore, Interface stiffness can be considerably increased by the process of loading and unloading would be reached because the slope of the unloading curve is larger than that of loading one. for the study pressure distribution was not studied.

Cabinets F. et al. [52] analyzed the tribological aspect of the surface topography variations for injection cams to study the repercussion of observed variations of surface topography on the tribological behavior of the cam roller contact. The study Used Greenwood- Williamson contact model. Result of the model showed that the flat part of the cams with a high number of peaks of sharp radii gives the worst tribological conditions. Furthermore, the running in is an unavoidable and beneficial effect on surfaces leading progressively to lower contact pressures. The base circle of the cam has a poor running-in and leads to higher pressures. In the study, contact stress between the cam and follower and Contact pressure of the system was not studied.

Megalingam A. A. and Mayuram M. M. [53] probed the effect of surface parameters on finite element method based deterministic Gaussian rough surface contact model to analyze the effect of surface parameters on a rough surface using 3-D contact analyses of Gaussian rough surfaces using finite

element method. Result of the study showed that for the surface having low surface roughness, the asperities deform mostly elastically and for the medium and high surface roughness surfaces, the elasto-plastic and plastic deformation of asperities are significant. The study also depicted that in low autocorrelation length surface, the intensification of subsurface stresses causes the mean contact pressure ratio to reach a peak value. In addition, in a high autocorrelation length surface, the larger size of asperities and the neighboring asperity interaction keep the mean contact pressure ratio at a low level. In the study, pressure distribution and Contact stress between the cam and follower was not studied.

Bayuseno A.P. et al. [8] utilize a FEM for modeling of real rough surface to model the real rough surface with a validation of the result with the experimental method. The study employed producing deterministic rough surfaces in ABAQUS by pre-processing on SOLIDWORKS using the curved wizard method. Result of the study depicted that the topography of the undeformed surface obtained (present model) is the closest to the experimental results. The resulting topographic deformed surface (present model) is the closest to the experimental results) with an error of 4.3%. Furthermore, the contact area that occurs after contact from the surface of the FEM results in the ABAQUS software is identical to the surface of the experimental results in a state of static loading. Contact body stress analysis (contact pressure and surface shear stress) and Contact body area was not studied.

Louay S. Yousuf and Nabil Hassan Hadi [54] studied the contact Stress Distribution of a Pear Cam Profile with Roller Follower Mechanism to study the effect of contact compression load on the contact stress distribution of the cam profile at the point of contact. The study used a theory of circular plate, FEM using ANSYS, modeling using SolidWorks, and experiment setup as a study methodology. The result depicted that the contact stress increased linearly with the increase of compression load. Furthermore, result of the study showed that the contact stress is maximum when the follower is located at 270° with the cam, while the contact stress is minimum when the follower is located at 180° with the cam at a compression load of 12.485 N. In the study, the effect of surface finish is not studied.

Sahoo and Chatterjee [55], present a study on elastic-plastic axi-symmetric hemispherical contact for a frictionless deformable sphere pressed by a rigid flat by using a FEA. The material of the sphere is modeled as elastic perfectly plastic. Analysis is carried out to study the effect of varying modulus of elasticity and sphere radius in wide range of dimensionless interference until the inception of plasticity as well as in plastic range. Results are compared with previous elastic-plastic models. It is found that materials with Young's modulus to yield strength ratio less than and greater than 300 show strikingly

different contact phenomena. The dependency of young's modulus on dimensionless interference at which the plastic region fully covers the surface is observed. However, with different radius, finite element study exhibits similar elastic-plastic phenomena.

Shankar and Mayuram [56], analyzed An axisymmetrical hemispherical asperity in contact with a rigid flat is modeled for an elastic perfectly plastic material. The study extends the work (sphere in contact with a flat plate) of Kogut–Etsion Model and Jackson–Green Model and addresses some aspects uncovered in the above models. This paper shows the critical values in the dimensionless interference ratios Y/E for the evolution of the elastic core and the plastic region within the asperity for different Y/E ratios. The present analysis also covers higher interference ratios, and the results are applied to show the difference in the calculation of real contact area for the entire surface with other existing models. The statistical model developed to calculate the real contact area and the contact load for the entire surfaces based on the FEM single asperity model with the elastic perfectly plastic assumption depends on the Y/E ratio of the material.

Saha and Jackson [57], perform a FEM to model to analyze the behavior of an elastic and elastic-perfectly plastic axisymmetric sinusoidal surface in contact with a rigid flat for a wide range of material properties and different values of the amplitude to wavelength ratio from initial to complete contact (high load). The numerical results agreed well with the Hertz model and the Jackson–Green elastic–plastic spherical contact model at low loads. Empirical equations for elastic and elastic-perfectly plastic cases are formulated for the contact pressure, contact area and surface separation. From the current analysis, it is found that it is not any single parameter, but different combinations of material properties and surface roughness that govern the whole contact behavior. The critical value of the amplitude of the sinusoidal asperity below which it will deform completely elastically from initial to complete contact is established. At low values of amplitude normalized by the critical amplitude, it was found that the contact behaved similar to a spherical contact, with the average pressure (hardness) always remaining lower than three times the yield strength. However, at higher values the average pressure increased toward a value as high as six times the yield strength at complete contact.

2.3 Literature Review Summary and study Potential

So far, different studies used numerical methods to investigate the effect of determining topography parameters on analyzing elastic contact between isotropic rough surfaces, numerical modeling of 3D rough surfaces to analyze interfacial contact characteristics and the contact behavior such as the pressure distribution, contact width, real area of contact and contact resistance of real rough surfaces. Various studies also tried to examine contact stress distribution on the cam profile, the effect of surface finish and surface coating on the maximum subsurface stress, and the impact of surface finish of cam on friction power loss. Furthermore, the effect of the machining process on the surface finishing of machined parts. Milling, turning, grinding operations final surface finish efficiency were demonstrated by experimental methods for gears, shafts, bearings, rings, and cams was analyzed.

However, different studies around the ignored the material property effects and the contacting body stress analysis in terms of contact pressure distribution, vertical stress, horizontal stress, and surface shear stress has not clarified. The effects of material properties with different density and surface finish on Moly based low alloy cam component subjected to contact load have not been studied numerically yet. Therefore, in this study two values of density of cam lobes, 7.35 g/cm^3 (Fe-1.5Mo-0.3C) and 7.55 g/cm^3 (Fe-1.5Mo- 0.2C) will used as a variable property of the material with same surface finish property. Furthermore, the low-density cam lobe (with density of 7.35 g/cm^3) analyzed for two different surface finishes, which are machined and powder metallurgy (PM) surface finished, to study the variation of surface finish on the same density of a material. The material is selected since the material is newly developed in the laboratory experimental study previously, thus density and surface finish parameters were recorded accordingly.

The above listed gaps in the previous studied is the motive to perform this study. Thus, this study work has the value of filling the gap of considering the effects of density difference and surface finish at the carburized cam surface by studying the maximum contact pressure, the real area of contact, pressure distribution, vertical stress, horizontal stress, and surface shear stress under varying load by using the numerical method utilizing ABAQUS software. The validation of the numerical method will be analyzed by using two distinct methods; the methodology validation by using previous similar study, and by implementing grid independent test on the performed simulation.

Chapter 3: The Research Methodology

3.1 Introduction

In this chapter, methodologies utilized for the study presented step-by-step. Selecting particular material with data collection; rough surface modeling; computational modeling of the problem using ABAQUS; and validation of the computational result performed to achieve the primary objective of the study. Methodologies used within the study presented in detail via the following subsections.

This section introduces the method employed for the study and details of numerical expressions of the overall modelling of static contact to achieve the research objective. Figure 3.1 show the schematic diagram of the conceptual framework of the applied methodologies. The main sections of the methodologies are:

(1) Material data collection
(2) Rough Surface Modelling
(3) Computational modelling of elastic contact using ABAQUS software.

Figure 3.1 Methodology Flow chart of the study

3.2 Material Data Collection

The material used in this study were carburized moly based low alloyed steel which is experimentally optimized material used for cam and follower. The material property is optimized and identified using density measurements performed by the water displacement method. The material is selected since the material is newly developed in the laboratory experimental study previously, thus density and surface finish parameters were recorded accordingly. The roughness data for the optimized material were measured and recorded [58]. The material property data used in this study presented in figure 3.2 via 3.4 and table 3.1 and table 3.2.

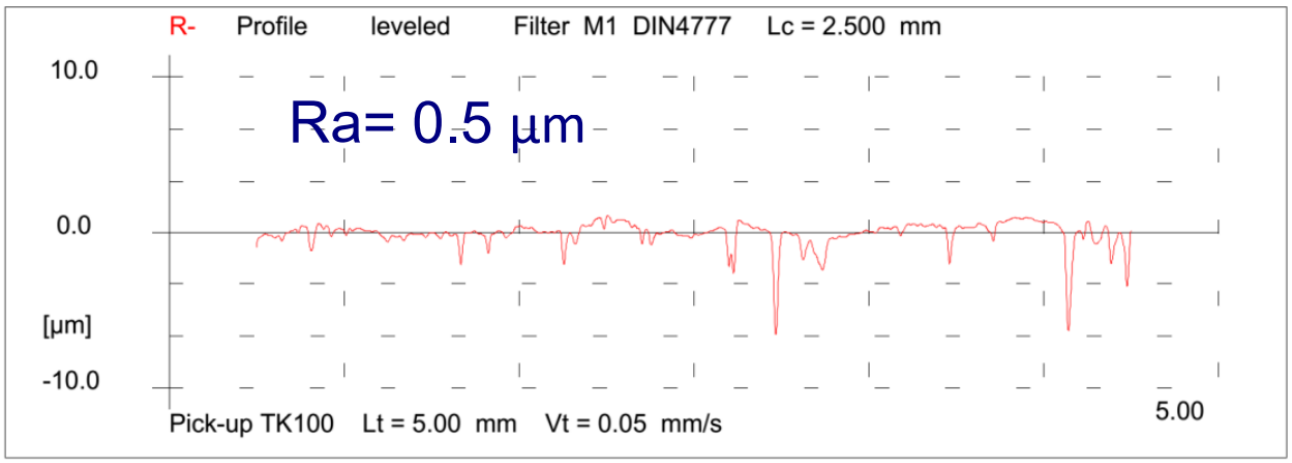

Figure 3.2: 7.35g/cm^3 PM surface finish [58]

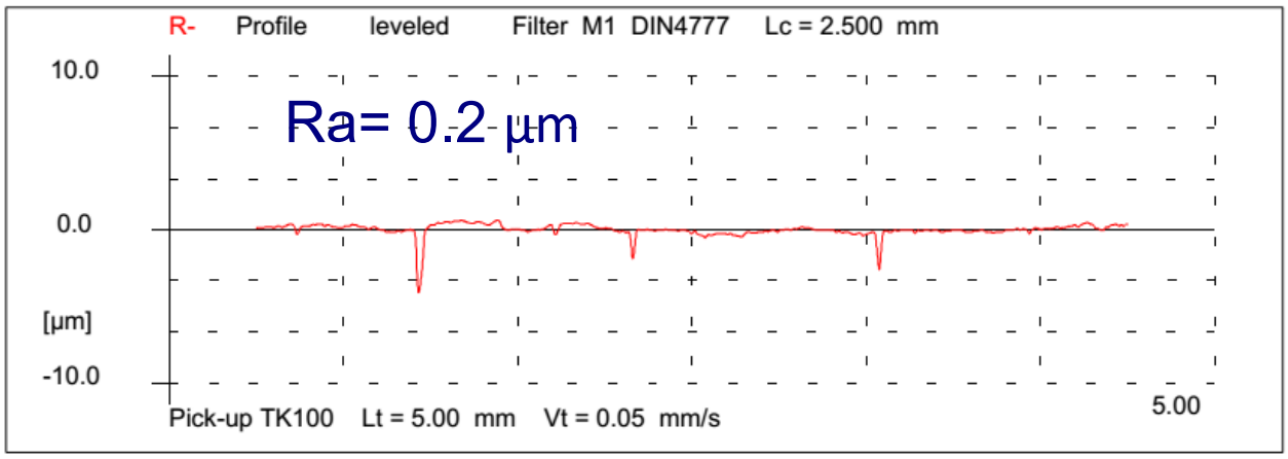

Figure 3.3: 7.35g/cm^3 Machined surface finish [58]

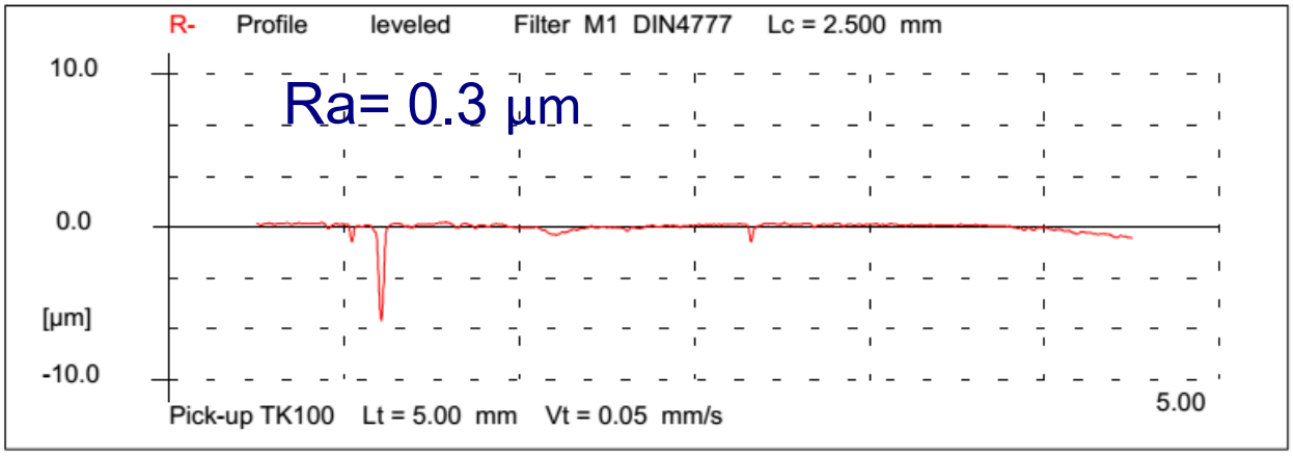

Figure 3.4: 7.35g/cm^3 PM surface finish [58]

N is the number of asperities in one surface, L_c is the sample length or cutoff length of the surface area and R_a is average roughness.

Table 3.1 Roughness parameters number of asperities, sample length and average roughness of the surfaces [58]

Surface no.	Manufacturing process	N	Lc(mm)	Ra(mm)
1	Low density- PM surface finish	110	2.5	0.0005
2	Low density – Machined	70	2.5	0.0002
3	High density - PM surface finish	55	2.5	0.0003

Table 3.2mechanical properties of the surfaces [58]

Surface	Density (g/cm^3)	Yield strength (MPa**)**	Elastic modules (GPa)	Poisson's ratio
low density – PM surface finish	7.35	1925	167	0.27
low density – machined surface finish	7.35	1925	167	0.27
High density – PM surface finish	7.55	1900	184	0.27

3.3 Rough Surface Modeling

3.3.1 Introduction

The first stage is to generate a rough surface using mathematical computations in the form of point clouds with the extension (*.xyz) that are generated at random. In XYZ format, a point cloud data file must have rows and columns of data. Each row in a rectangular coordinate system must contain the X-, Y-, and Z-coordinates, as well as the field value at that point. These point clouds were then converted into three-dimensional (3D) models using SolidWorks software. A data file called a Parasolid (*.x t, *.x b) is used to exchange 2D or 3D design information between CAD programs. The Parasolid extension (*.x t, *.x b) or other extensions compatible with FE software were changed by

using solid work software. ABAQUS commercial software is used to simulate static contact on a rough surface.

The method is a combination of mathematical, CAD and FE software

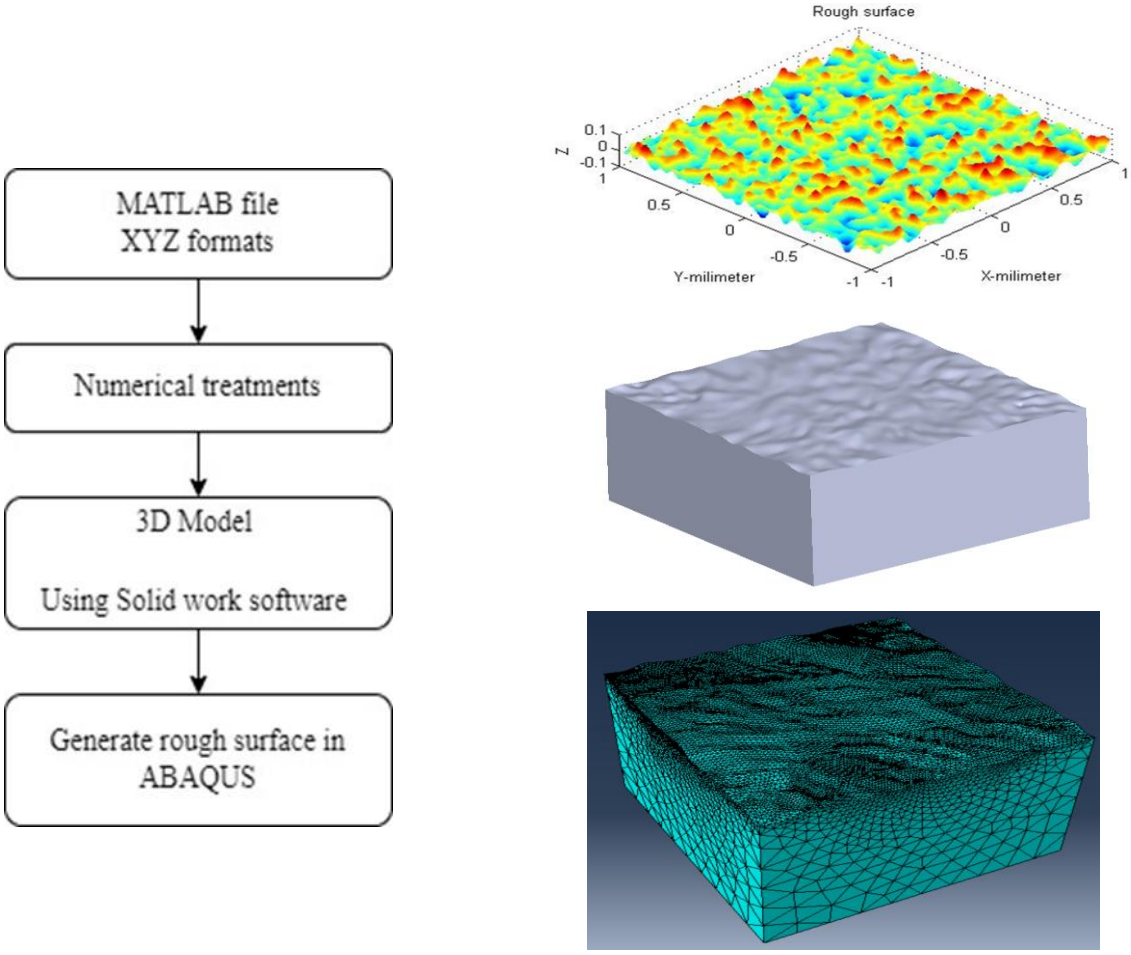

Figure 3.5: Methodology for generating rough surface

3.3.2 Simulation of Rough Surfaces With FFT

The rough surface in this study was constructed using mathematical software and based on a mathematical equation. To create a surface with random roughness, Gaussian equations were employed. In this study, generate random surfaces by using FFT. Because the frequency domain approach and FFT algorithms are the most efficient way to perform filtering operations. The direct convolution filtering technique is straightforward but inefficient in terms of processing speed [6–8].

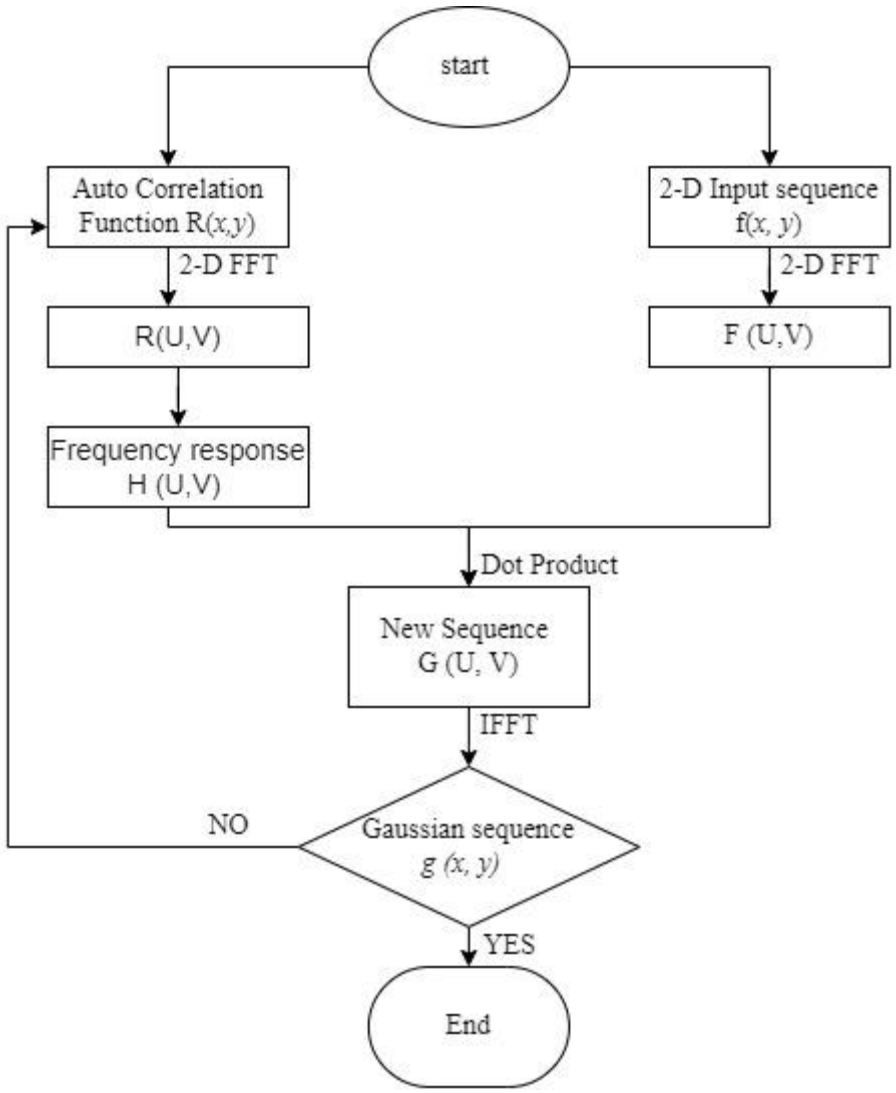

Figure 3.6: Numerical simulation of Gaussian random surfaces.

The following processes are used to simulate a random surface

1. Generate 2-D input sequences $f(x,y)$. the components of $f(x,y)$ are independent gaussian distributed random numbers.

$$f(x,y) = f = e^{-\left[\frac{(x^2+y^2)}{2\sigma^2}\right]}$$

Where, x and y are a row vectors which linearly spaced in the length of the surface area.

2. Specify the autocorrelation function $R(x,y)$ of the simulated surfaces according to assuming expressions of engineering surfaces.

$$R(x,y) = \sigma^2$$

3. Compute the 2-D fast Fourier transform (FFT) of $f(x,y)$ obtaining the sequence $F(u,v)$

   2-D fast Fourier transform are generated in MATLAB by command $fft2$

$$F(u,v) = F = fft2(f)$$

4. Compute the 2-D fast Fourier transform (FFT) of $R(x,y)$ obtaining the sequence $R(u,v)$

$$R(u,v) = fft2(\sigma^2)$$

5. Determine the frequency response of the filter $H(u,v)$

   Random number whose element are normally distributed with transfer functions are generated in MATLAB by command $randn$. The mathematical expression is

$$H(u,v) = H = fft2(\sigma .* randn(N,N))$$

6. The new sequence $G(u,v)$ is generated from the dot product of the sequences $H(u,v)$ and $F(u,v)$.

$$G(u,v) = fft2(H) .* fft2(F)$$

7. Compute the 2-D inverse discrete fast Fourier transform IFFT of the sequence $G(u,v)$ obtaining the output Gaussian sequence $g(x,y)$.

   2-D inverse discrete fast Fourier transform are generated in MATLAB by command $ifft2$

$$g(x,y) = ifft2(fft2(H) .* fft2(F))$$

Based on the aforesaid process, the model was pre-processed in MATLAB (appendix A, B and C) and emerged in a two-dimensional form. The generated surface's coordinate surface data was transformed (Fig. 3.7). The resulting surface data was then exported to the "XYZ" format, which contains X, Y, and Z values for each point. The "XYZ" data was converted to a surface array format. There are several variables in the GHD equation that can be applied into a mathematical program. N is the number of asperities in one surface, L_c is the sample length or cutoff length of the surface, Ra is average roughness and σ is height of the root means square (rms). For a gaussian random profile the relationship between R_a and σ for a Gaussian random profile is given in equation 2.34 in the previous chapter.

Table 3.3 Root mean squares of the surfaces

Surface no.	Manufacturing process	Rms(mm)
1	Low density- PM surface finish	0.00063
2	Low density – Machined	0.00025
3	High density - PM surface finish	0.00037

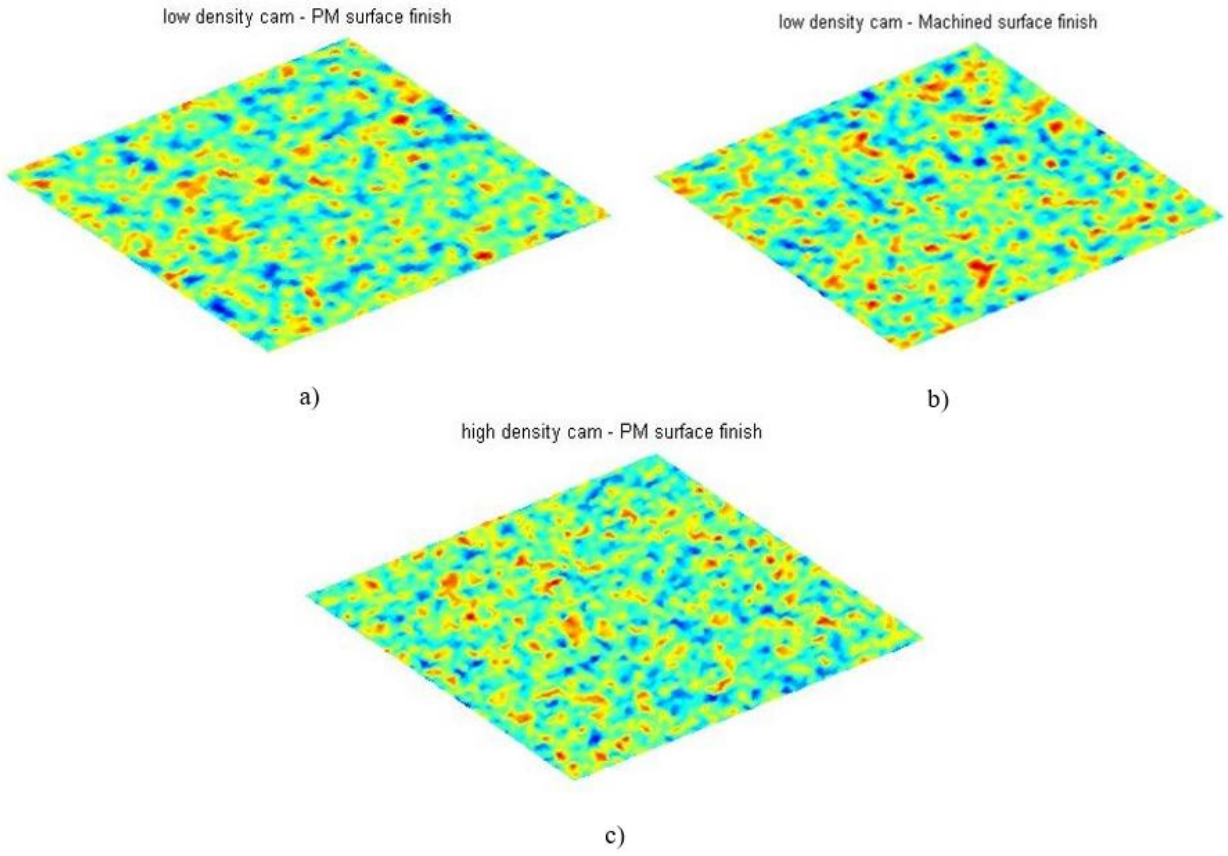

Figure 3.7: Rough surface plot a) with low density cam - PM surface finish, b) with low density cam - Machined surface finish and c) with high density cam - PM surface finish

3.3.3 Development of Solid Surface on SOLIDWORKS

3.3.3.1 Importing Point Clouds

A cloud of points is imported into the software, which represents an embedded set of coordinates (x, y, z) of points on a three-dimensional surface. The matrix function is used to create the cloud of points necessary for CAD/CAE system import of the model surface. From the cloud of points, a three-

dimensional object must be created in CAD systems, and then the object geometry must be imported into the CAE system. In some cases, the problem can be simplified to an axisymmetric or two-dimensional form, allowing the importation of only the surface profile's x and y coordinates, which are dependent on the set of x and y values. By using SOLIDWORK software can be transform the coordinate (*x*, *y*, *z*) into a solid surface by connecting each coordinate from the surface array. After opened the file "XYZ" on SOLIDWORK the file was changed into point clouds (Fig.).

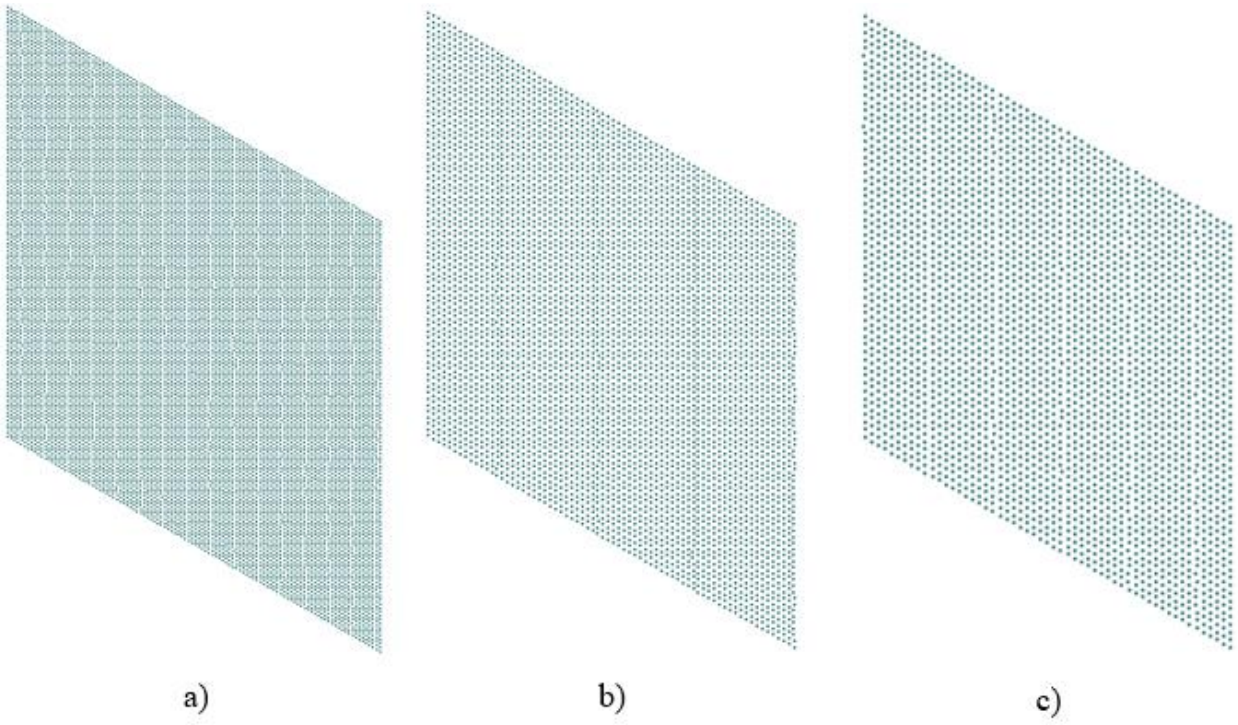

Figure 3.8: point cloud a) low density cam - PM surface finish, b) low density cam - Machined surface finish and c) high density cam - PM surface finish

3.3.3.1.1 Curve wizard

Curve wizard is a surface-making technique that involves cutting a point cloud into many planes. In the methods of automatic and guided generation, the curve wizard method was used without the mesh process. This study uses automatic creation because in solid/surface creation during generating process, automatic creation provides better control the shapes of faces and result smoother surface than guided creation. Without skipping the reduction amount process, the curve wizard uses a point cloud as a base for creating solid surfaces.

3.3.3.1.2 Solid Model

In MATLAB, the measurement's resultant surface containing the points is plotted. Metrics are produced as a result of graphing the points. The second plot of the Surface points on SOLIDWORKS is then created, with as many points as necessary to produce a perfect curve surface such as Figure 3.9. In MATLAB, the surface generated was plotted with up to 12100 for a, 5041 for b and 3025 for c points. The results of the graphing are utilized to create a curve.

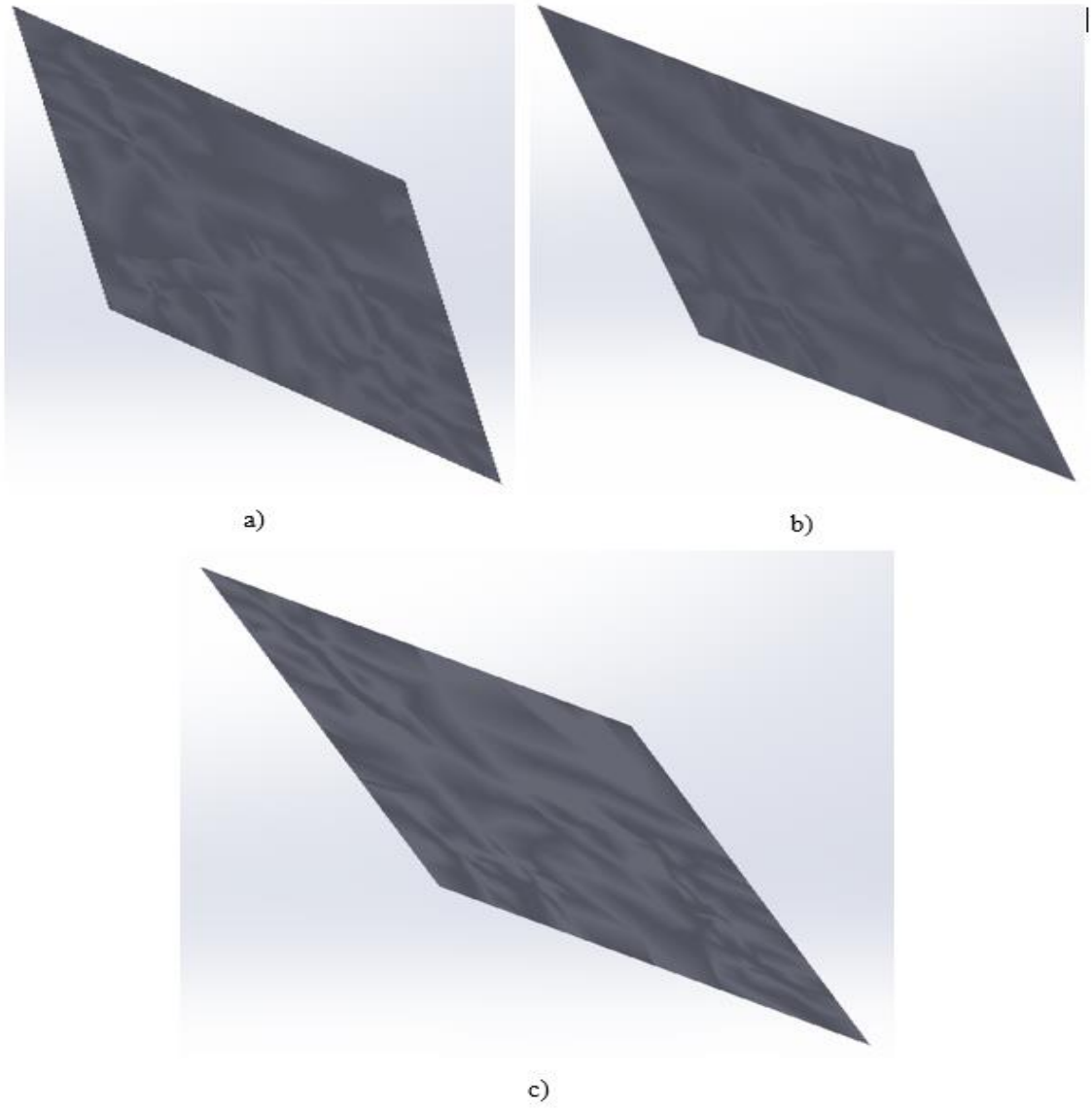

Figure 3.9: Surface model a) low density cam - PM surface finish, b) low density cam - Machined surface finish and c) high density cam - PM surface finish

3.3.3.1.3 To extrude on rough surface

The number of nodal "XYZ" formed finer surfaces throughout the solid surface generation procedure. The surface is then given thickness, making it resemble the true model in Fig.

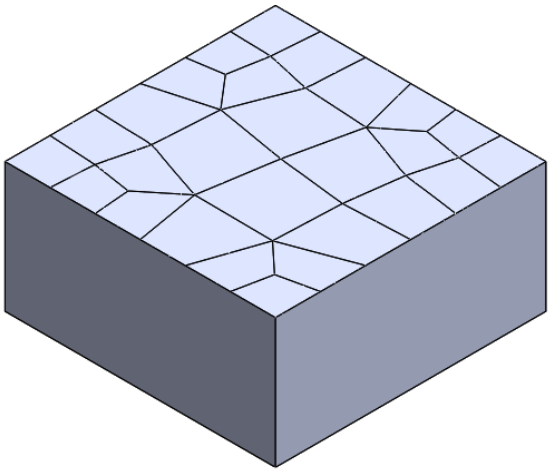

Figure 3.10: Extruded rough surface

3.4 Modelling details of finite element analysis package used for the contacting problems.

3.4.1 Introduction

The methodology for elastic contact modeling with the Abaqus finite element software is described in this section. Contact conditions are regarded a specific parameter of discontinuous constraint behavior in finite element analysis, allowing nodal forces to be transmitted from one model part to another. Because it is only used when the two-part surfaces come into direct touch, this constraint has a discontinuous situation. When the two model portions are separated, there is no need for such a constraint. As a result, the contact analysis must determine when and where two surfaces are in contact and apply the appropriate contact constraints.

3.4.2 The Abaqus CAE software package

Pre-processing which is an interactive CAE activity, simulation which involves utilizing Abaqus/Standard and Abaqus/Explicit and post-processing which involves visualizing the finite element analysis results using the Abaqus viewer tool. The modeling process started with the model of a rough surface and smooth follower geometry model.

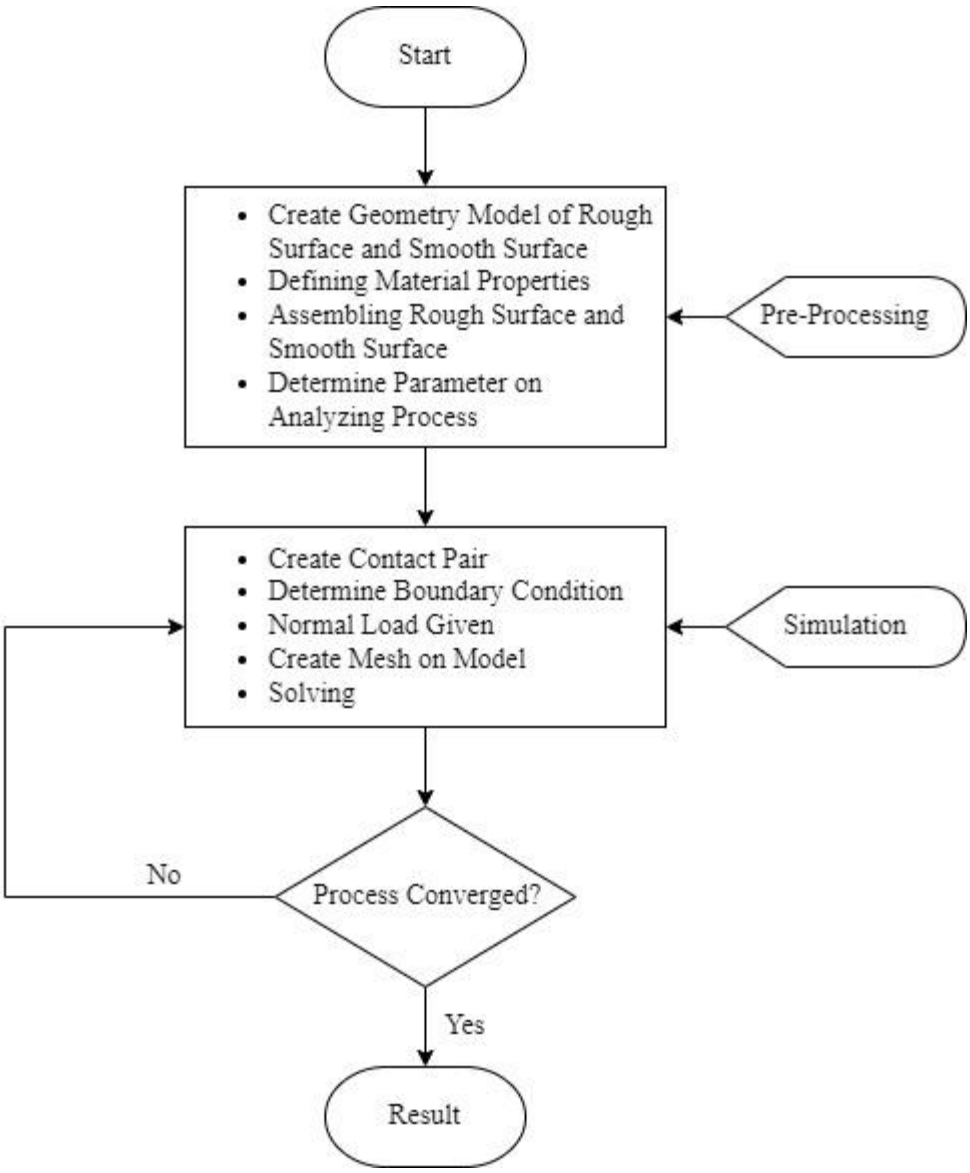

Figure 3.11: Flow chart modeling on FEM ABAQUS

3.4.3 Pre-processing stage

This stage is a pre-processor that interacts with the user to create the finite element model. In addition, with the accompanying input file, a model of the physical contact problem is created. This can be accomplished with the help of the graphical tools included in the CAE program. In addition, an Abaqus input file analysis can be readily constructed using a text editor. The discretized part shape, mechanical properties, boundary conditions, type of analysis, and element type are all defined at this stage.

3.4.4 Simulation with Abaqus/standard

The finite element issue defined in the model is solved by Abaqus/Standard or Abaqus/Explicit at this stage. Because of the uncertain contact area and elastic plastic parts, this is a nonlinear problem that must be solved iteratively. In preparation for post-processing the output data is saved in binary files. The simulation time is determined by a number of factors, including the complexity of the contact problem to be solved, computer system requirements, and computer power usage. For the reasons stated above, the analysis provided in the input file may take anything from minutes to several hours to complete.

3.4.5 Post- processing (visualizing the finite element analysis result)

The results are usually visualized interactively using Abaqus/Viewer, which gives a graphical representation of the analysis. The fundamental variables for presentation, such as displacements, stresses, and forces can be provided at this stage. Animation tools, deformed and undeformed shape plots, contour plots, material orientations, and harmonic animation are some of the possibilities for displaying the results in Abaqus/Viewer.

3.5 Computational Modelling of surface contact on Abaqus /CAE software

For finite element analysis Abaqus/CAE provides a complete modeling and visualization environment. The result may be conveniently managed and created, edited, monitored, diagnosed, and visualized by users. Abaqus/CAE is organized into modules, each of which describes a logical aspect of the modeling technique.

Modeling and presentational tools in Abaqus can be used with a variety of methodologies and strategies. The buttons located alongside the modeling viewport can be used to access the majority of the basic modeling features. Within Abaqus/CAE, there are a variety of modeling tools.

3.5.1 Part module

To proceed with the Finite Element modelling, the model must be imported as a part into ABAQUS after being generated with SOLIDWORKS software. ABAQUS allows you to import and export a variety of files. There are a variety of file formats that the software may read in order to store data related to geometry. In this work, chooses the Parasolid format for importing parts and sketches. Unigraphics, SOLIDWORKS, Solid Edge, FEMAP, and MSC.Patran are just a few of the CAD programs that can create Parasolid-format parts.

The first step to import Parasolid files into ABAQUS is save the part in SOLIDWORKS in a "(*.x_t*,*.x_b*, *.xmt*)" format. We must import the part into ABAQUS after it has been stored in a new format.

All models have two parts, the rough cam surface and the smooth follower. The rough cam surface generated using MATLAB and SOLIDWORK and after that imported into ABAQUS. The second part smooth roller follower modelled using SOLIDWORK software and and imported into ABAQUS.

Table 3.4: Dimensional of contact part

Part name	Modeling space	Type	Feature shape	Feature type
Rough body	3D	Deformable	Solid	Planer
Smooth rigid body	3D	Rigid	Solid	Planer

3.5.2 Property module

The property model can be used and specified by the Abaqus user to accomplish the following tasks: material definition, section assignment, and part orientation. A section must be assigned to each part or model. The material property is the geometry that has been applied to the part. The material property used here is elastic material with density, young's modulus E and poison's ratio v.

Table 3.5: Dimensional and material characteristics of all parts [58]

Case	Material behavior	Type	Density (g/cm^3)	Young modules (MPa)	Poisson's ratio	Section type
low density – PM surface finish	Elastic	Isentropic	7.35	167e3	0.27	Planer
low density – machined surface finish	Elastic	Isentropic	7.35	167e3	0.27	Planer
High density – PM surface finish	Elastic	Isentropic	7.55	184e3	0.27	Planer

3.5.3 The step module

The purpose of the step processes is to determine the type of analysis that will be performed in the ABAQUS program. In addition, the field output request tool allows the user to specify which outputs

are required in each analysis stage of the simulation, as well as the area of the model from which they will be output. In places where considerable element distortion occurs during analysis, this module is also used to construct adaptive mesh regions and set controls for adaptive meshing. Static analysis is the type of analysis used in this study. Step procedure as in table

Table 3.6: Static step module analysis parameter

Step	Step name	procedure	Time period	Increment size			Max. number of increments
				Initial	minimum	maximum	
0	initial	initial	N/A	N/A	N/A	N/A	N/A
1	Apply load	Static, general	1	1	0.00001	1	100000

3.5.4 Interaction module

By selecting possibly interacting surfaces and defining the approach in terms of how the Abaqus package will deal with them, this module is used to define and control interactions between different parts in an assembly or between a specific section of a model and its surroundings. Surface-to-surface contact, self-contact, and general contact are the mechanisms used by Abaqus to analyze and deal with interactions.

In this case, contact interaction refers to the interaction of smooth rigid body surfaces with a rough surface. The rigid surface of the follower is referred to as the master surface, while the rough surface is referred to as the slave surface. The friction formulation of the contact interaction is rough.

Table 3.7: Interaction property of rough surface with smooth surface

Interacting part	Interacting type	Contact property	Normal behavior	Contact formulation
Rough surface with Smooth surface	Surface -to-surface	Tangential behavior	Hard/soft contact	Rough

3.5.5 Load module

This module specifies the type of loading and application region, and also determine the boundary conditions. Model parts can be loaded with a variety of load cases, loads, predefined fields, and boundary conditions. Depending on the desired load, a load can be a force, a pressure, a time, and so on. Displacement, rotation, velocity, and other boundary conditions can be used.

The model is concentrated normal forces applied to the displacement degrees of freedom Loaded in Y direction at the center of rigid body as shown in Figure 2.5. To be able to simulate the master slave simulation it is important that the BC's (Boundary Condition) are chosen in a proper way. Therefore, the rigid body movements in the X stand Z direction are suppressed and rotations around the Y axis vector is free as well and the simplified slave is fixed at the bottom in all directions.

Table 3.8: Load condition

Load type	Location	Load at step
Normal load	At the center of rigid body	[100 up to 10000] N

3.5.6 Mesh module

This module contains tools that allow the user to specify mesh properties and mesh density to generate and control finite element meshes on parts created in Abaqus/CAE. In addition, the mesh tool allows the user to choose an element form and meshing approach, generate a mesh and seed a component instance that fits the problem's requirements. To evaluate mesh quality based on element shape and check for numerical analysis problems, the mesh module employs a range of finite element approaches. The part is partitioned before meshing by separating the asperities zone from the bottom of the part. When meshing accurately, separating the asperity zone reduces the overall number of elements generated substantially. Types of elements used C3D6 (A 6- node linear triangular prism).

Meshi procedures:

I. Global seeds: entire surface sized 0.025length/element.
II. Local seed: giving the size on rough surface with the length 0.02/element.
III. Mesh controls: select wedge (C3D6) as types of the element shape
IV. Mesh part instance: click to run mesh process then the result as on the picture below

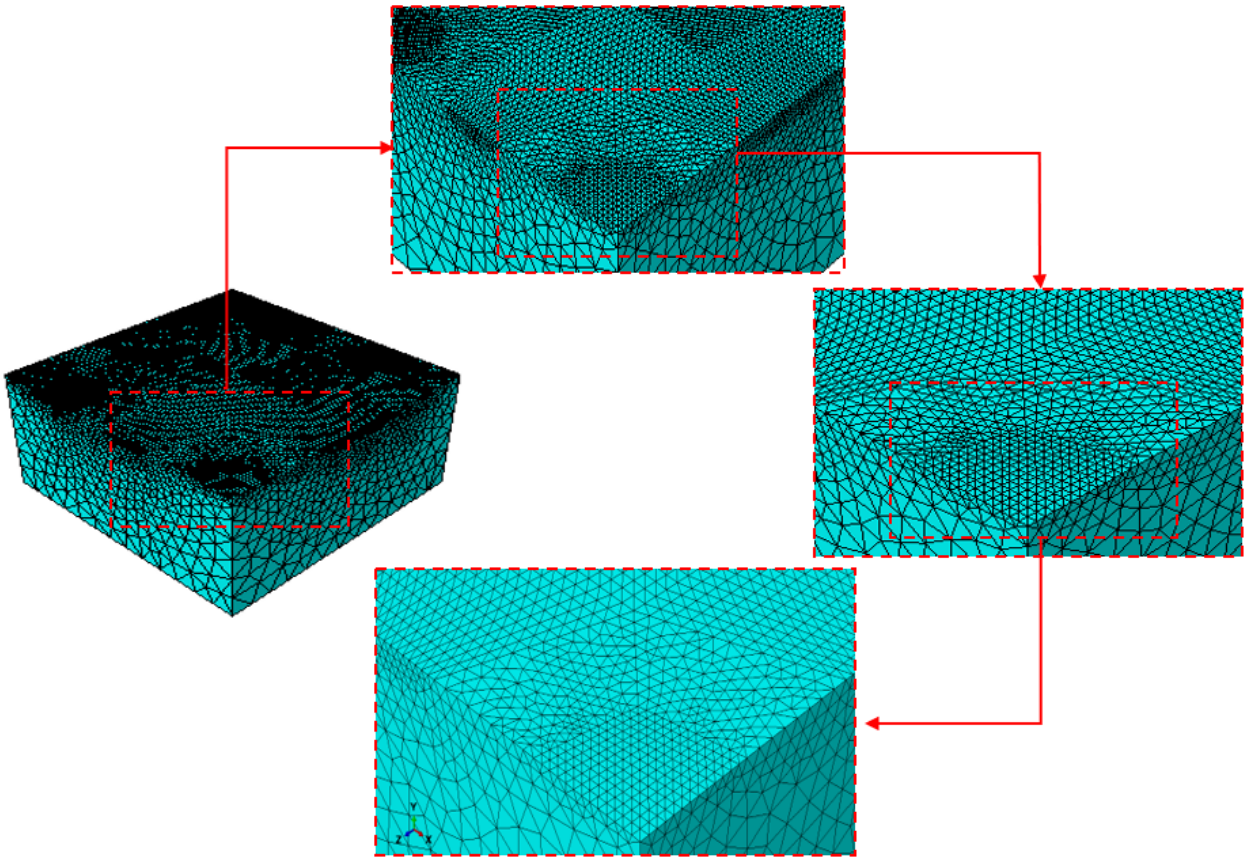

Figure 3.12: Surface after being meshed

3.5.7 Job

When the user has completed all of the task requirements including defining a model for analysis, defining the geometry of the model, applying load, assigning material properties, and defining the type of contact, the Job module is used to submit and analysis a model of the problem. In addition, this module is beneficial in terms of managing the analysis and viewing a basic plot of the analysis results, checking and monitoring progress of the execution of the analysis job.

3.5.8 Visualization

This module provides graphical display for the results of a job analysis, in particular, contour plot on the deformed shape, and a symbol plot. The other benefits of this module are its ability to control and specify what information is required to be placed in the output database, scale factor animation and history or x-y data.

3.6 Mesh Independent Test

Finite element numerical methods are is a potent tool for simulating a variety of challenging real-world problems. However, the success of finding a solution does not guarantee numerical accuracy. When the number of finite elements in the model is more, the solution is more accurate. Nevertheless, how accurate is it? Is there a rule to decide the level of accuracy in the solution? How can we achieve accuracy? Those questions must get an answer to determine the minimum grid size or mesh resolution required to solve the problem by using FEM.

To show the problem's solution in the study is accurate adaptive mesh convergence techniques were performed in all the study cases. This technique allows the minimization of errors and uncertainties in the predicted results. Adaptive convergence requires the problem to be solved multiple times with different mesh discretization sizes, namely starts with coarse mesh move to finer mesh.

Table 3.9give the mesh dependent test for PM surface of a contacting bodies and follower contact with different number of elements at the same applied load which is 100N.

Table 3.9: Mesh dependent test result

Num. of Element	Max. contact pressure (MPa)
5868	257
8438	520.1
11046	741.1
19925	1323
29038	1563
34320	1697
42463	1843
56600	2011

71962	2122
85850	2334
94636	2466
97688	2519
106004	2605
130645	2631
162927	2651

The maximum contact pressure variation curve of the contacting bodies under the application of 100N load obtained using different element discretization also presented in Figure 3.13.

It is seen that; the value of maximum contact pressure for the last two element sizes become almost the same. The relative error used to determine the per cent change of pressure between the consecutive mesh densities. In this case, the relative error is measured as zero. This phenomenon gives a clear insight that the FEM implemented is independent of the mesh size in all cases.

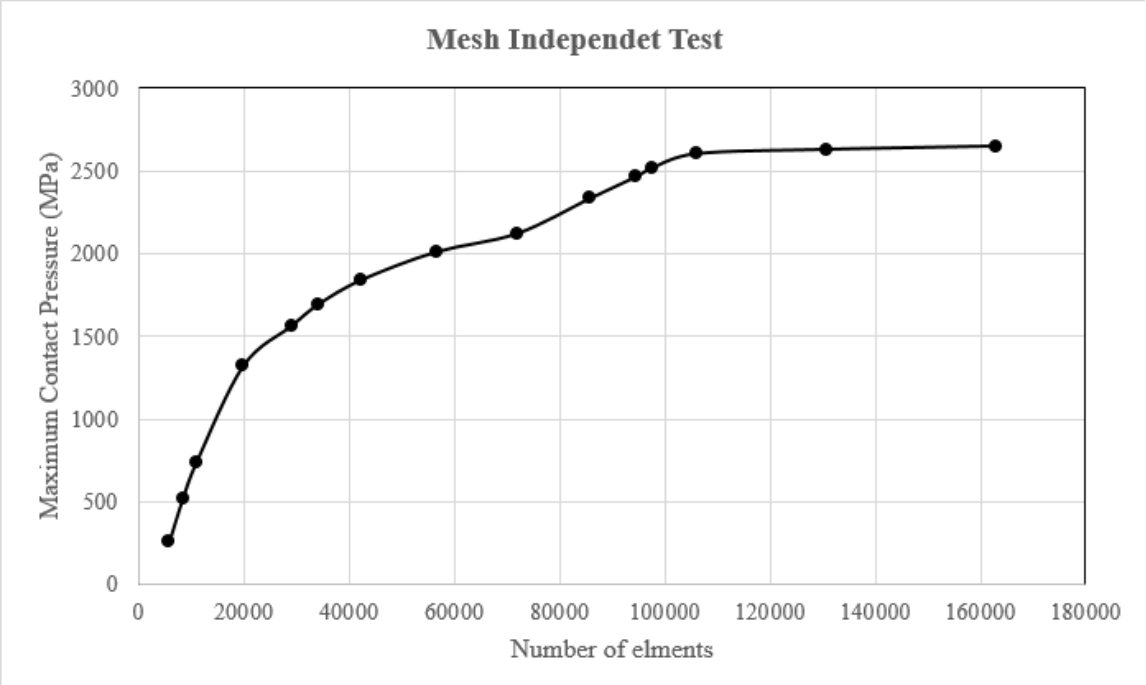

Figure 3.13: Mesh Independent Test

3.7 Validation of numerical approach

The contact parameter results of the Gaussian rough surface model with a rms of 0.1 mm are taken into consideration in order to validate the current numerical approach. Loading is initially supported by a single asperity only. The current multi-asperity numerical technique can be validated by observing the behavior of this dominant single asperity. The resulting real area of contacts of the applied contact load by the single asperity are extracted from the contact model discussed above. The generated MATLAB function is used to determine the peak radius of this single asperity. The contact load and actual contact area of the identified single hemispherical asperity in contact with a rigid flat are determined by using the Hertz elastic. Table 3.10 shows the contact area variation of the current numerical approach with the Hertz solution. It is noted that the variation of the current numerical method and the Hertz solution result is within the permissible range of error (below 3%) for the given contact load as indicated in previous studies [53].

Table 3.10: Validation of present numerical approach with Hertz approach

Contact load (N)	Contact area (mm^2)	
	Numerical model	Hertz solution
250	0.0031885	0. 0030958
500	0.0064932	0.0063985
1000	0.0113501	0.0109932

Chapter 4: Result and Discussion

4.1 Simulation Results

Based on the solution, solved results for all models obtained. Using the above established contact models, this section aimed to revealing the contact characteristics comprises of the maximum von mises stress, the contact pressure distribution and the real contact area at different load levels based on the finite element analysis of all rough surface models.

4.1.1 Effect of surface finish method on contact parameters

In incremental steps, all generated deterministic rough surface contact models are analyzed. For every incremental step, the contact parameter results are extracted. The normal contact load is applied in the normal direction (along y direction). By adding the elemental areas of the contact elements which bear the contact load, the real area of contact is obtained. The maximum Von mises stress and maximum contact pressure are found from the nodal values. By dividing the applied contact load by the real contact area, the average contact pressure value is determined.

At low load, the faces made contact at only a few points on the surface and the area of the contacts was quite small. Numerous sections show no interactions at all. As the load was increased, the number and area of contacts raised. By evaluating the total area of contact on Abaqus as a proportion of the surface's area, the dimensionless area of contact was determined. This proportional area was taken to be equal to the nominal contact area for the entire surface. At each applied load level, the relative contact area, A_r/A, was calculated by averaging the measurements from Abaqus. The load is normalized by dividing by nominal area of contact and the elastic modulus (E).

4.1.1.1 Real contact area

The variation of dimensionless real area of contact with dimensionless contact load is given in Figure 4.1.

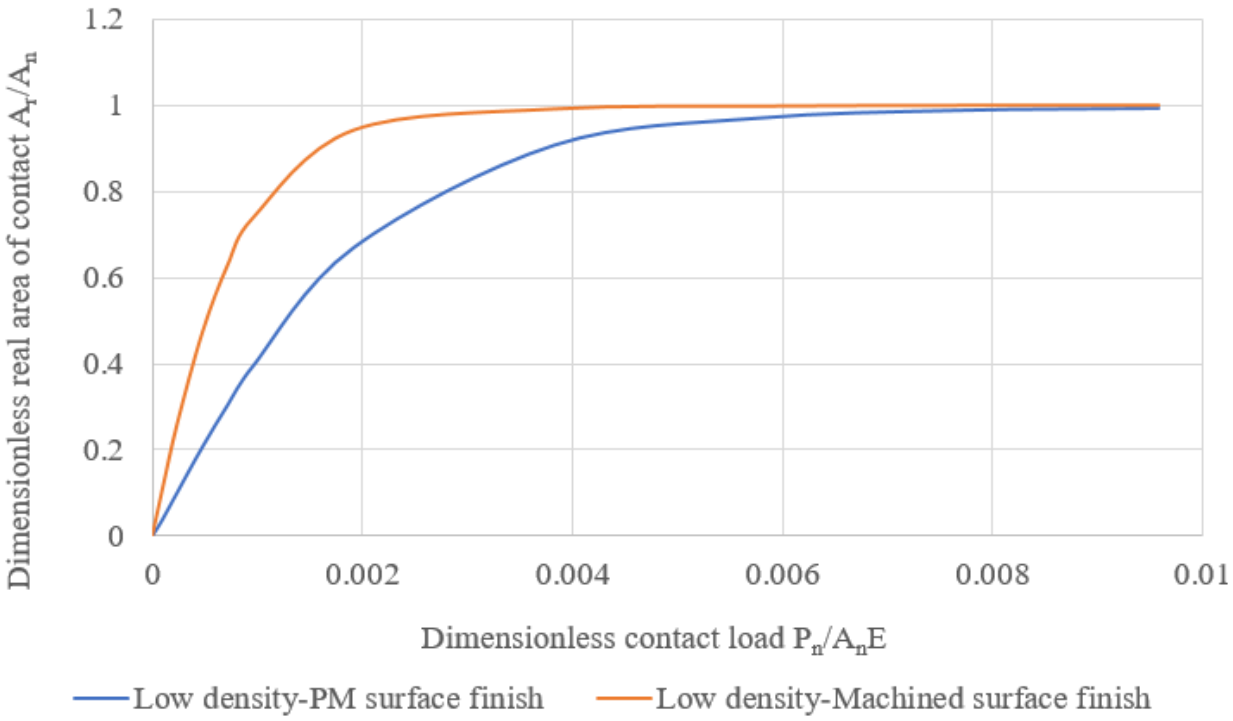

Figure 4.1 Variation of dimensionless real area of contact with dimensionless contact load

Figure 4.1 shows the variation of dimensionless real area of contact with dimensionless contact load for both the rough surface contact models (low density-PM surface finish and low density- machined surface finish) with varying surface finishing method. As the dimensionless contact load increases, the number of contact point and the dimensionless real area of contact also increases in a nonlinear or exponential manner in the both cases and lower the average roughness R_a value, then higher is the contact area. Due to small size of average roughness, rough surface having large size of asperities and also exhibits high dimensionless real area of contact. To attain the same dimensionless real area of contact, PM surface finish rough surface has to take additional contact load due to large average roughness value even though the number of asperities is high.

4.1.1.2 Mean and maximum contact pressure

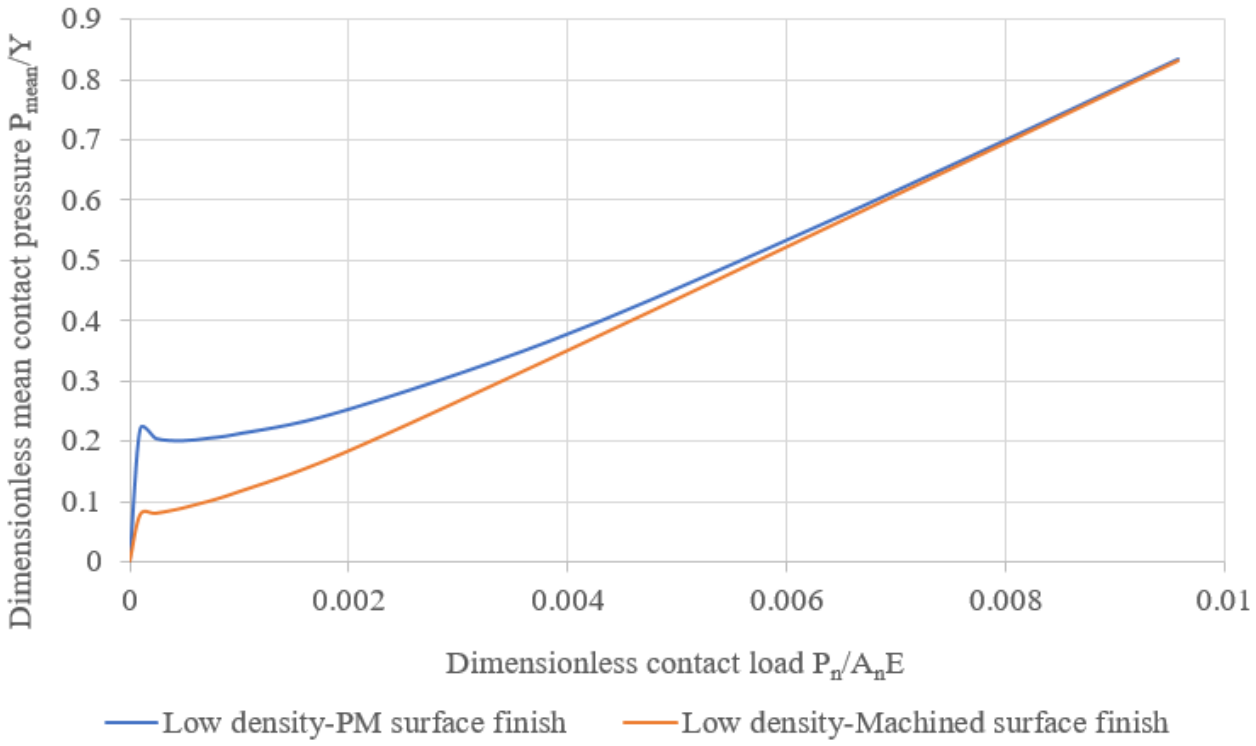

Figure 4.2 shows the variation of dimensionless mean contact pressure with the dimensionless contact load for rough surface contact models with varying method of surface finishing.

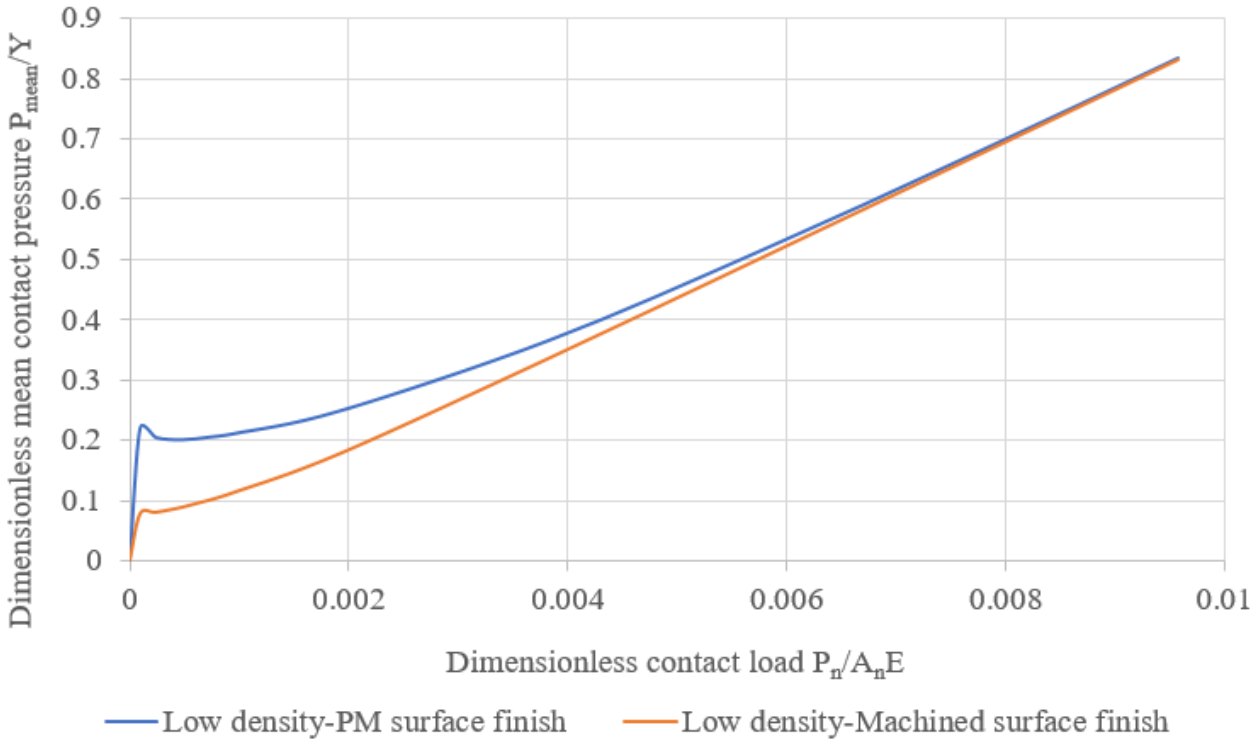

Figure 4.2 Variation of dimensionless mean contact pressure with dimensionless contact load

As the dimensionless contact load increase the dimensionless mean contact pressure increase for both rough surface cases. For the same dimensionless contact load, the PM surface finish surface shows a relatively higher mean contact pressure compared to machined surface finish rough surface. The rate of mean contact pressure (slope) is almost the same for the two rough surfaces. For the same material property (elastic modulus, poisons ratio, density), the mean contact pressure increases as the average roughness increase.

Figure 4.3 shows the variation of dimensionless maximum contact pressure with dimensionless contact load for both the rough surface contact models.

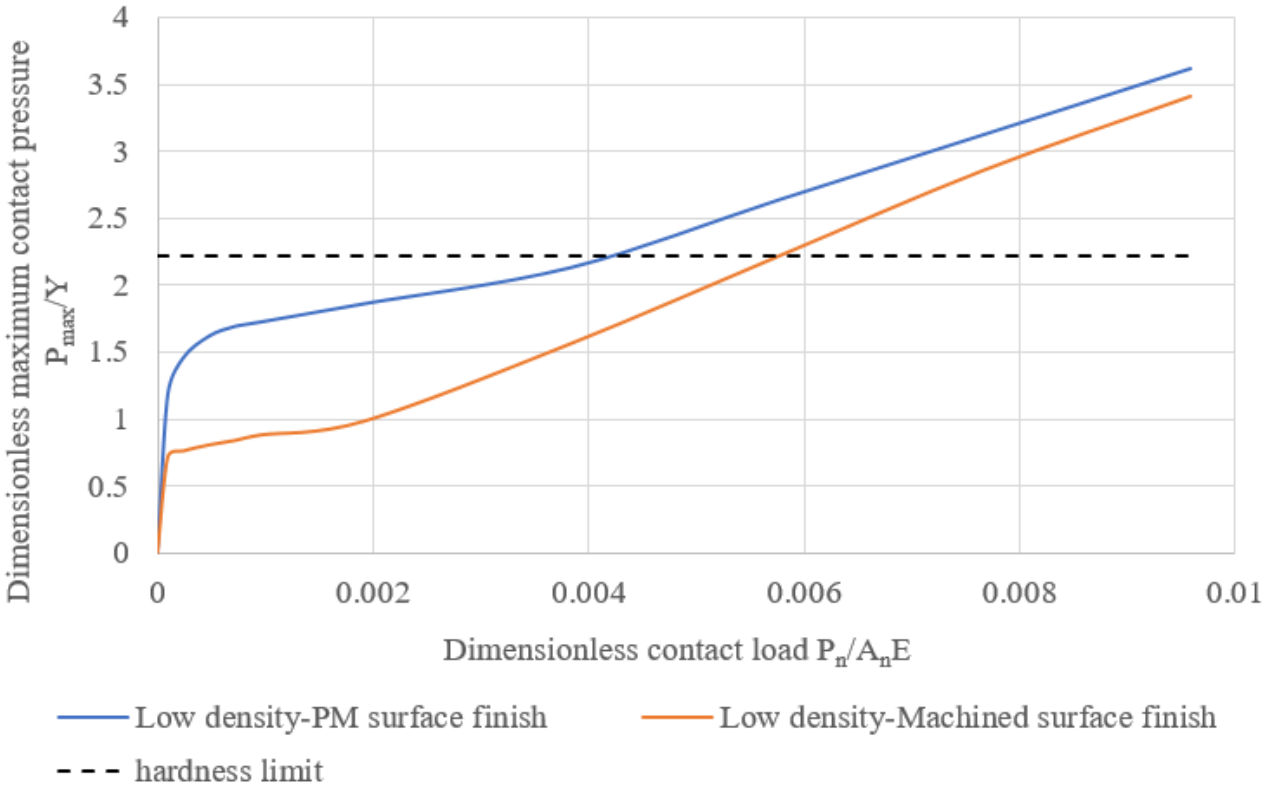

Figure 4.3 Variation of dimensionless maximum contact pressure with dimensionless contact load

Each rough surface contact model crosses or reaches its saturation level at a different dimensionless contact load. A keen observation shows that as the average roughness decreases, the required dimensionless contact load to cross the hardness limit value of 2.22 (as indicated by Shankar and Mayuram [56] and Sahoo and Chatterjee [55]) increases. In the PM surface model, the P_{max}/Y ratio to cross the hardness limit of 2.22 at $P_n/A_n E$ of 0.0042 and in the machined surface model the P_{max}/Y ratio to cross the hardness limit of 2.22 at $P_n/A_n E$ of 0.0057. The P_{max}/Y ratios of all the rough

surfaces are increasing beyond the hardness limit as the dimensionless load increases. Similar variation is noted in Bhushan [24], where there is an increasing trend in the maximum contact pressure beyond the hardness limit for various applied loads. The machined surface finish rough surface model reaches the hardness limit earlier compared to the PM surface finish rough surface model because in the former rough surface model (PM surface finish), the contacting area is small and the asperities are severe plastic deformation. The relationship between real area of contact, average contact pressure and maximum contact pressure with applied normal load is consistent with what is commonly observed in engineering practice. Therefore, by utilizing a machined surface finishing technique, plastic deformation can be avoided.

4.1.1.3 Von mises stress and contact pressure distribution

The Figure 4.4 shows the computed result of the effect of surface finish method on the von Mises stress for the above two models. The Figure 4.5 show the contact pressure distribution plot of the above two models.

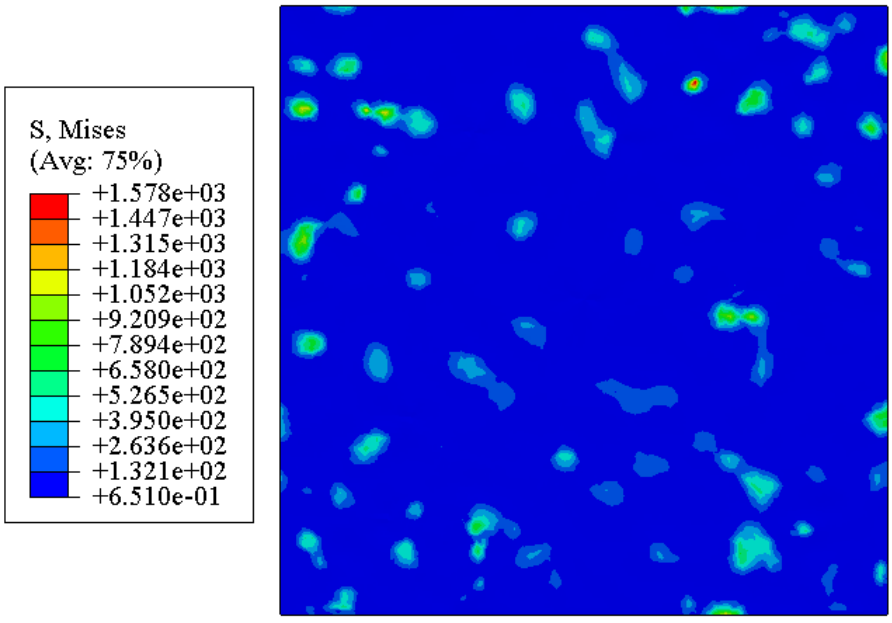

a)

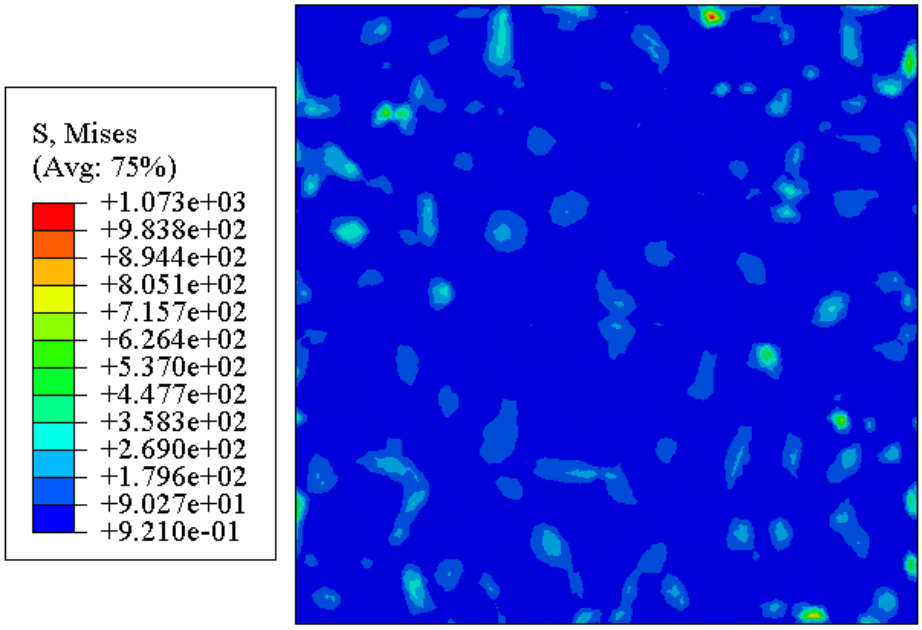

b)

Figure 4.4 Von Mises stress plot at load of 250N, a) PM surface finish b) Machined surface finish

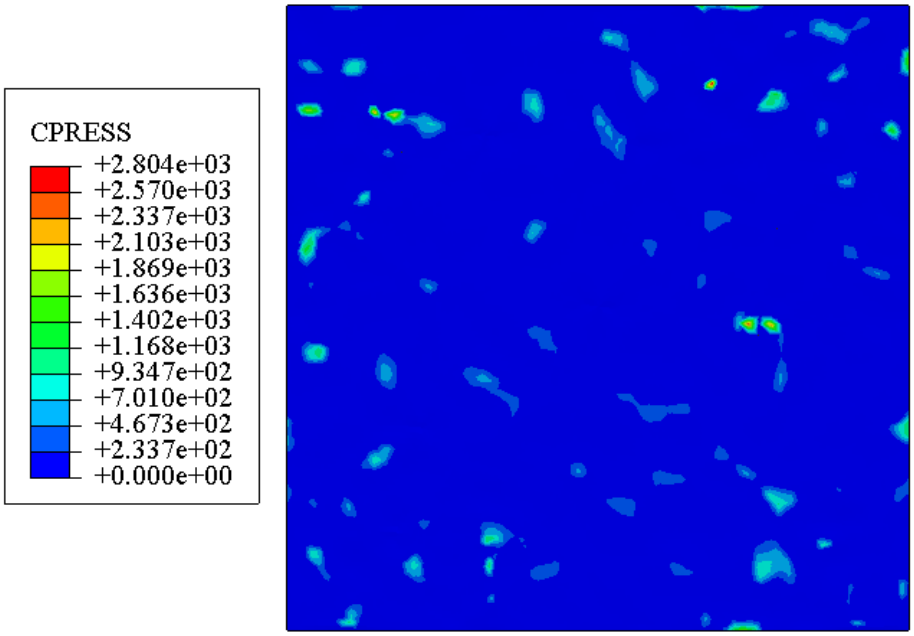

a)

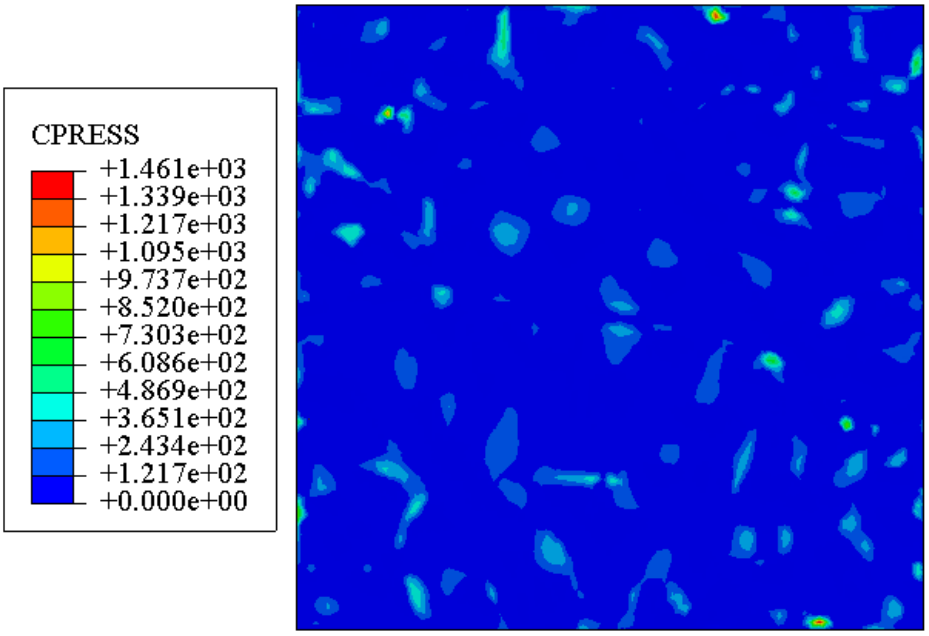

b)

Figure 4.5 contact pressure distribution plot at load of 250N a) PM surface finish b) Machined surface finish

Figure 4.4(b) show more asperity interaction compared to first model at the same contact load. The Figure 4.5(b) shows a greater number of asperity contacts compared to another model. It confirms that the machined surface finish model has a greater number of asperity interaction compared to PM surface finish model. The real contact area is low and the von mises stresses and contact pressure are high for the PM surface finish surface with Rms = 0.00063mm as compared to machine surface finish surface with Rms = 0.00025mm. For the surface with Rms = 0.00063 mm, real contact area occurs at 0.6377mm^2 or 10.2% of nominal contact area, the maximum von mises stress value is 1578MPa and maximum contact pressure value is 2804MPa. For the surface with Rms = 0.00025 mm, real contact area occurs at 1.6392mm^2 or 25.2% of nominal contact area, the maximum von mises stress value is 1073MPa and maximum contact pressure value is 1461MPa.

Figure 4.6 shows the contact surface after the random gaussian height distribution applied to a real surface. In this case, the variation in the surface is imperceptible to the naked eye. Figure 4.7 shows the computed result the contact pressure distribution under various applied contact load.

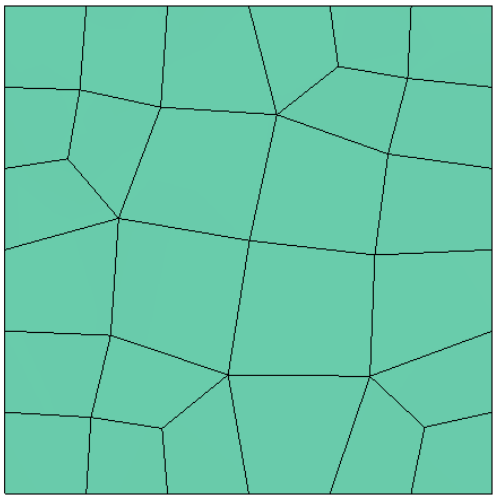

Figure 4.6 Rough surface (low density PM surface finish)

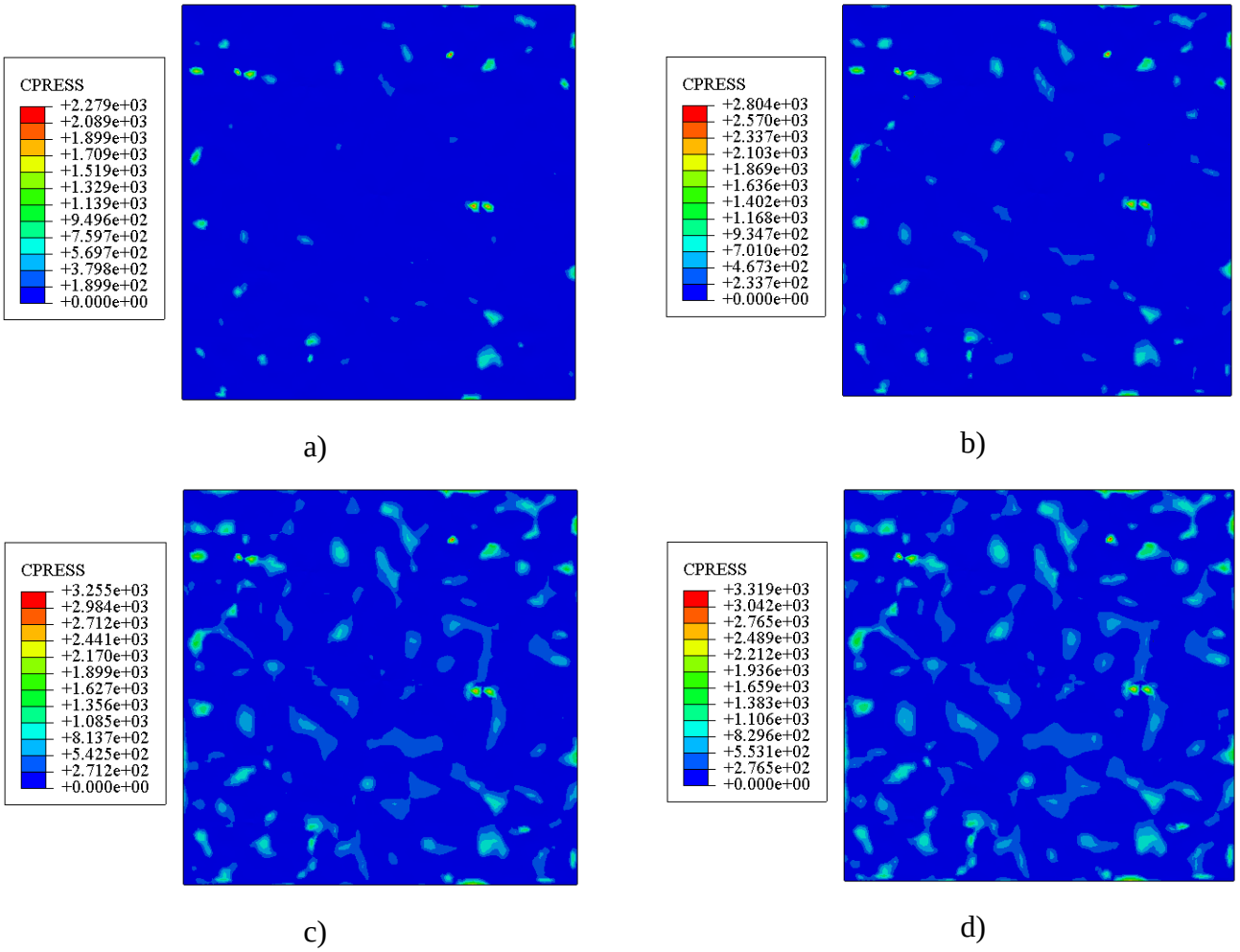

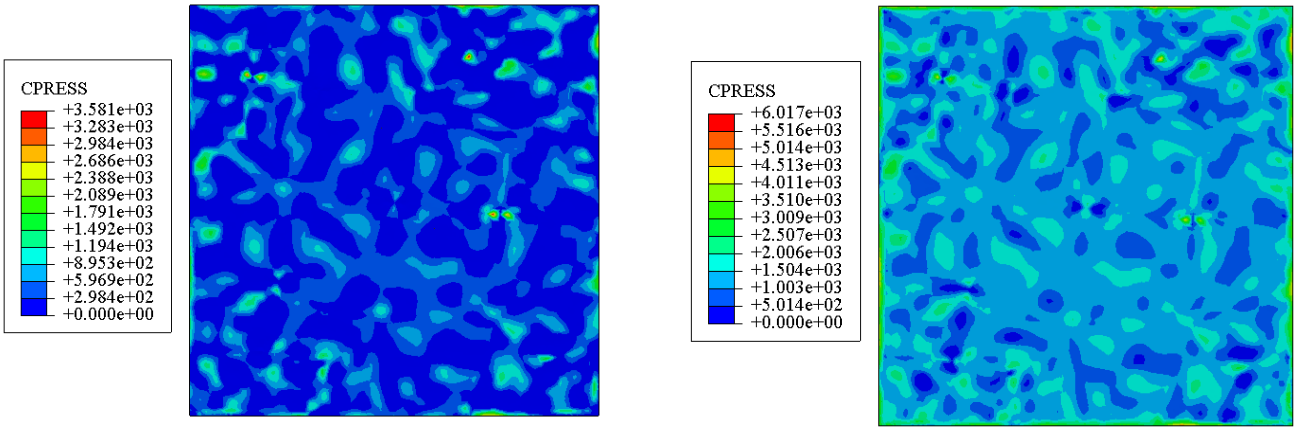

e) f)

Figure 4.7 Contact pressure map at a) 100N, b) 250N, c) 750N, d) 1000N, e) 2000N, f) 8000N and low-density PM surface finish surface

The contact pressure profile obtained from these six-contact load surface contact analyses are plotted in Figure 4.7. Applying a load 100N to the top surface of the upper rigid body generates a contact pressure distribution. For much of the surface the blue color shows that contact is not occurring. These small numbers of contact points are due to the small applied load. At the small load of 100N, real contact area covers 3.77% of nominal contact area, the maximum von mises stress value is 1322 MPa and maximum contact pressure value is 2279 MPa. At the mid load of 4000N, real contact area covers 90.88% of nominal contact area, the maximum von mises stress value is 2573MPa and maximum contact pressure value is 4102MPa. For high load of 8000N, real contact area covers 99.52% of nominal contact area, the maximum von mises stress value is 3787MPa and maximum contact pressure value is 6017 MPa. As the load increase, the contact pressure increases and the amount of the surface in contact (real contact area) also increases.

4.1.2 Effect of Material Density Variation on Contact Parameters

4.1.2.1 Real contact area

The variation of dimensionless real area of contact with dimensionless applied contact load for both the rough surface (low density-PM surface finish and high density-PM surface finish) contact models is shown in Figure 4.8.

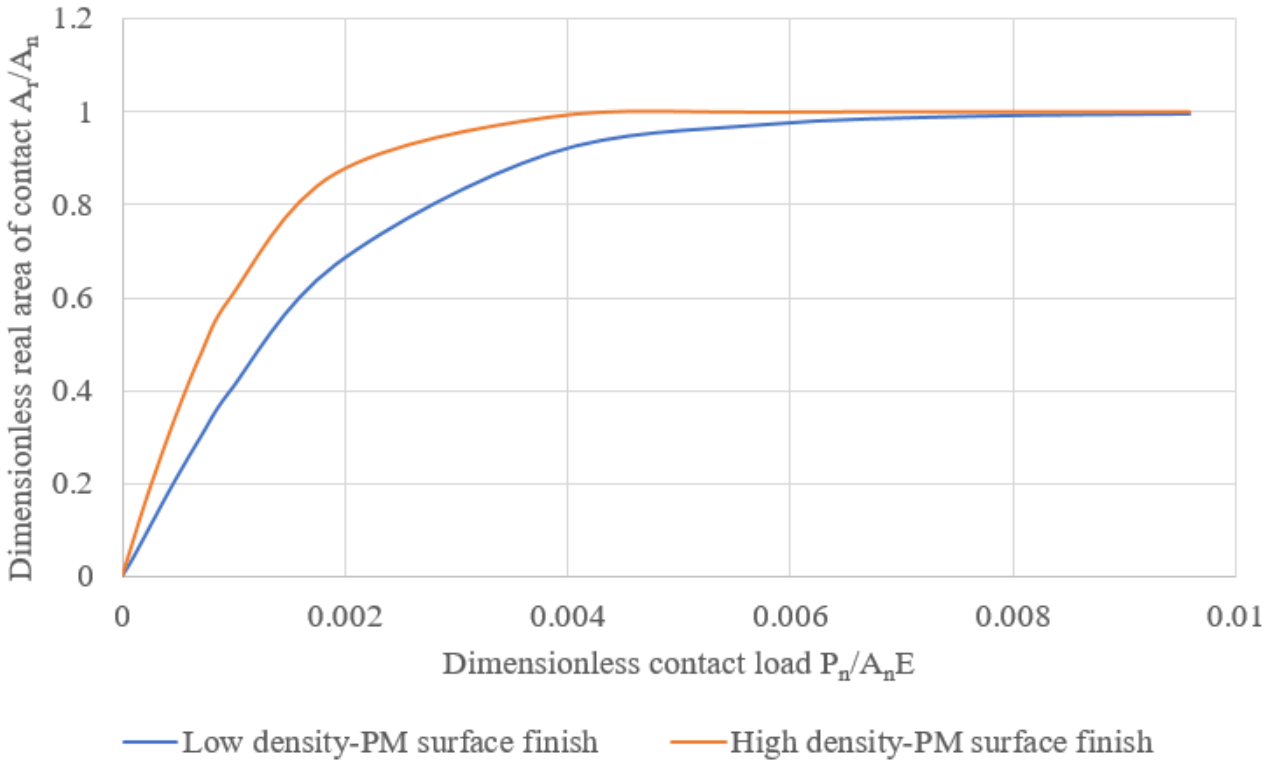

Figure 4.8 Variation of dimensionless real area of contact with dimensionless contact load

Dimensionless real area of contact and total number of contact points both increase in a nonlinear with dimensionless normal contact load increase as expected. For both rough surfaces, the rate of contact load increase (slope) is extremely similar. For the same dimensionless contact load, the higher density surface shows a relatively high real contact area compared to low density surface. Due to small value of average roughness and high elastic modulus, rough surface having large size of asperities and also exhibits high dimensionless real area of contact. To attain the same dimensionless real area of contact, lower density surface has to take additional contact load.

4.1.2.2 Mean and maximum contact pressure

Figure 4.9 shows the variation of dimensionless mean contact pressure with the dimensionless contact load for rough surface contact models with varying material density.

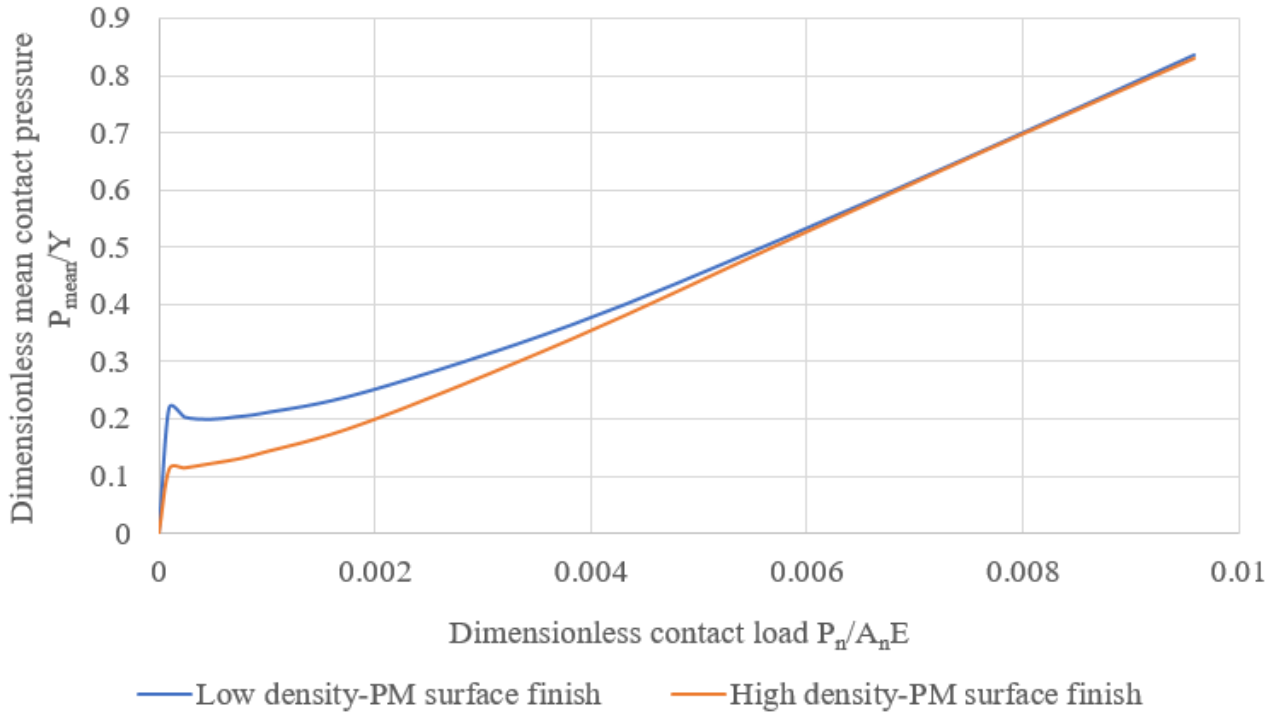

Figure 4.9 Variation of dimensionless mean contact pressure with dimensionless contact load

As the dimensionless contact load increase the dimensionless mean contact pressure increase for both rough surface cases. For the same dimensionless contact load, the low-density surface shows a relatively higher mean contact pressure compared to high density surface. The rate of mean contact pressure (slope) is almost the same for the two rough surfaces. For the same surface finishing method, the mean contact pressure increases as the material density decrease.

Figure 4.10 shows the variation of dimensionless maximum contact pressure with the dimensionless contact load for rough surface having two different material density.

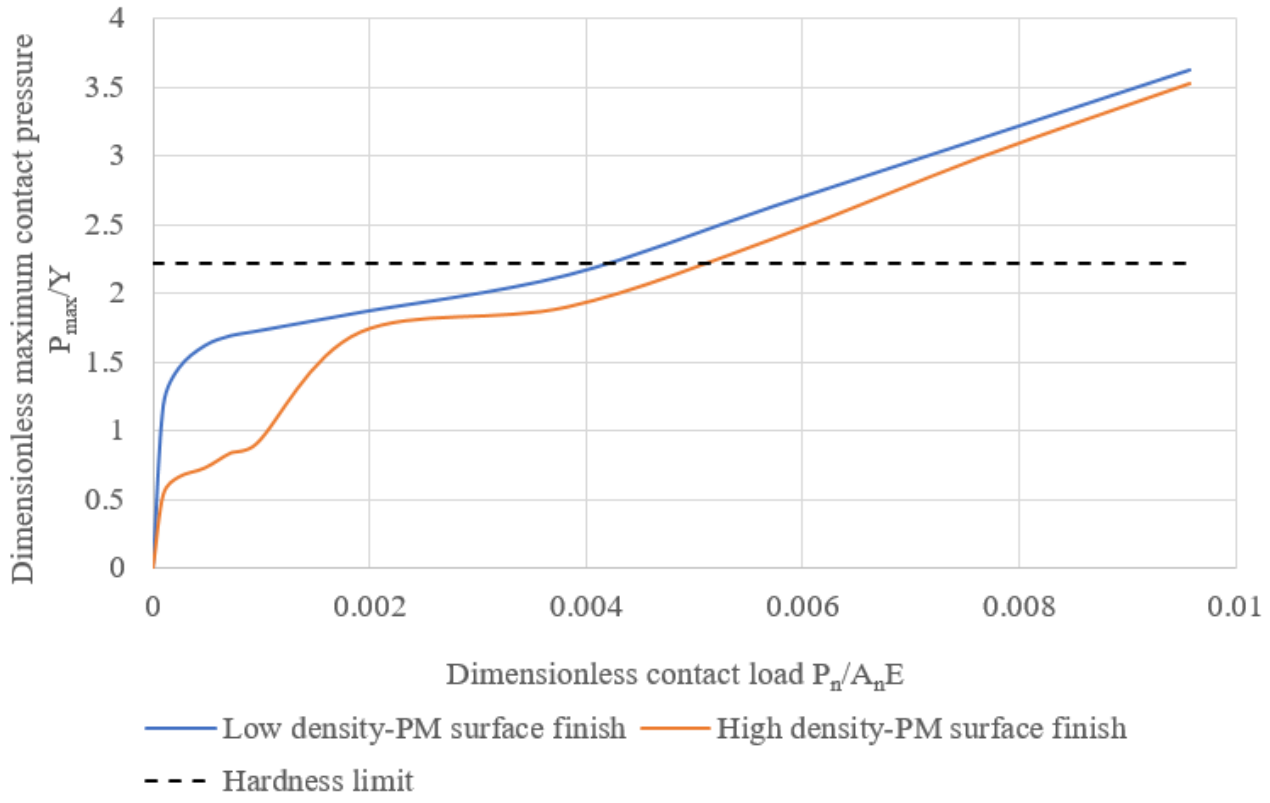

Figure 4.10 Variation of dimensionless maximum contact pressure with dimensionless contact load

Each rough surface contact model reaches its hardness limit at a different dimensionless contact load. A keen observation shows that as the material density increase, the required dimensionless contact load to cross the hardness limit value of 2.22 (as indicated by Shankar and Mayuram [56] and Sahoo and Chatterjee [55]) increases. In the low-density surface model, the P_{max}/Y ratio to cross the hardness limit of 2.22 at $P_n/A_n E$ of 0.0042 and in the high-density surface model the P_{max}/Y ratio to cross the hardness limit of 2.22 at $P_n/A_n E$ of 0.0051. The P_{max}/Y ratios of both rough surfaces are increasing beyond the hardness limit as the dimensionless load increases. The high-density rough surface model reaches the hardness limit earlier compared to the low-density rough surface model because in the high-density rough surface model, the elastic modulus is higher and make relatively small value of average roughness value. The relationship between maximum contact pressure with applied normal load is consistent with what is commonly observed in engineering practice.

4.1.2.3 Von mises stress and contact pressure distribution

The Figure 4.11 shows the computed result of the effect of density variation on the von Mises stress for two surface models (low density-PM surface finish surface and high density-PM surface finish surface). The Figure 4.12 show the contact pressure distribution plot of the above two models.

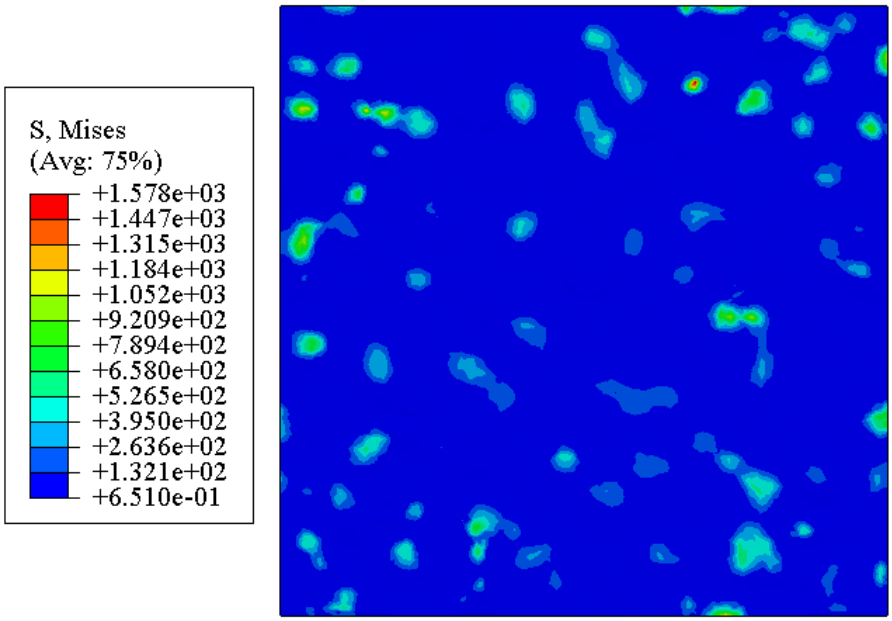

a)

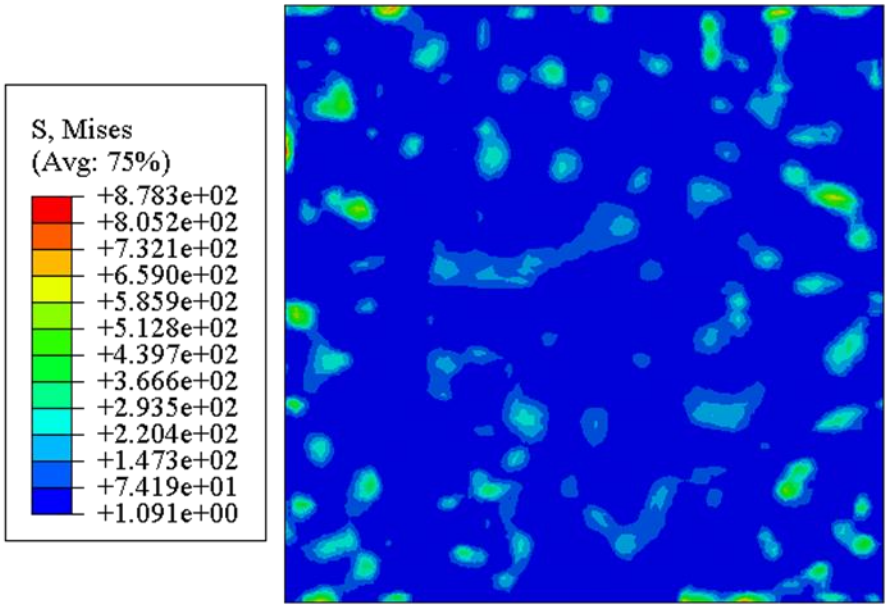

b)

Figure 4.11 Von Mises stress plot at load of 250N, a) low density PM surface finish b) high density PM surface finish

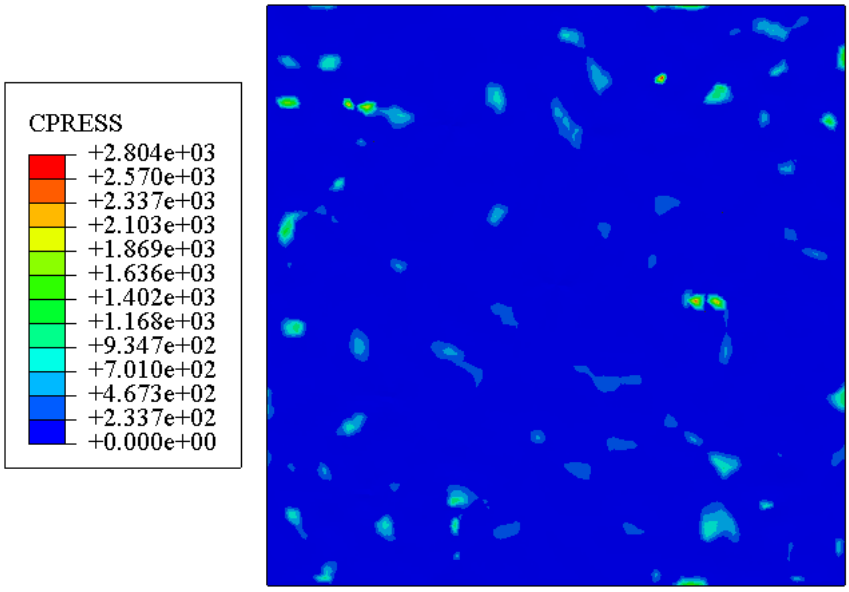

a)

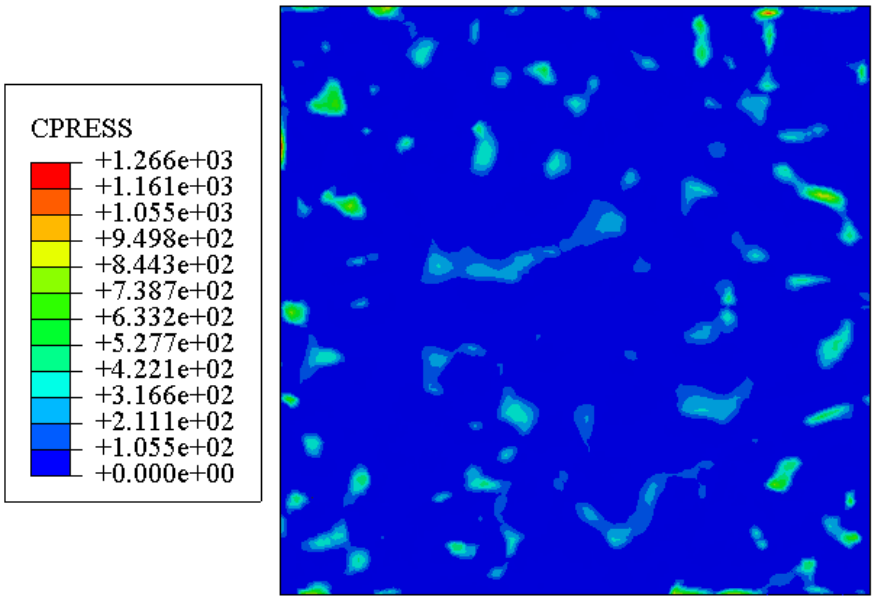

b)

Figure 4.12 contact pressure distribution plot at load of 250N, a) low density PM surface finish b) high density PM surface

Figure 4.11 (b) show more asperity interaction compared to first model at the same contact load. The Figure 4.12Figure 4.5(b) shows a greater number of asperity contacts compared to another model. It confirms that the low-density surface model has a greater number of asperity interaction compared to high density surface model. The real contact area is low and the von mises stresses and contact

pressure are high for the low-density surface with ρ = 7.35g/cm^3 as compared to high-density surface with ρ = 7.55g/cm^3. For the surface with ρ = 7.35g/cm^3, real contact area occurs at 0.6377mm^2 or 10.2% of nominal contact area, the maximum von mises stress value is 1578MPa and maximum contact pressure value is 2804MPa. For the surface with ρ = 7.35g/cm^3, real contact area occurs at 1.14115 mm^2 or 18.25% of nominal contact area, the maximum von mises stress value is 878.3MPa and maximum contact pressure value is 1266 MPa.

4.1.3 Effect of elastic modulus

The effect of elastic modulus is observed by varying the elasticity value. The variation of dimensionless real contact area with normalized contact load is shown in Figure 4.13.

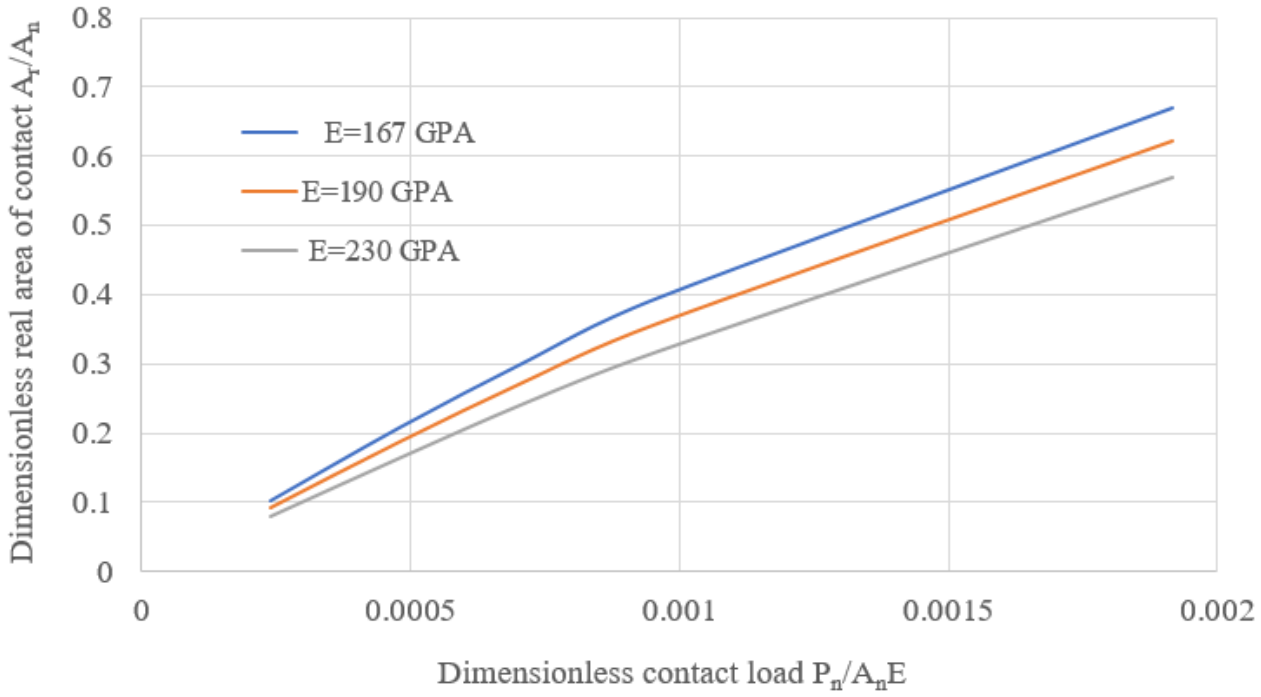

Figure 4.13 Variation of dimensionless real contact area with dimensionless contact load

Figure 4.13 shows the dimensionless real contact area relation for different value of Young's modulus (E= 167 GPa, 190 GPa, 230 GPa) at a rms of 0.00063mm and Poisson's ratio of 0.27. For constant dimensionless contact load, the surface modeling with high elastic modulus bears lower contact area compared to low elastic modulus surface. The behavior seen in Saha et al [57], also observed in the current analysis. In the work of Saha et al [57], it is seen that the amount of contact pressure necessary to achieve total contact steadily increases with an increase in Young's modulus. The analysis of the effect of Young's modulus shows that the amount of force needed to make complete contact increases with the higher the value of Young's modulus

Chapter 5: Conclusion and Recommendation

5.1 Conclusion

The aim of this study was to investigate the effect of surface finish and material properties on the carburized Moly based low alloy cam subjected to contact load using the numerical method. different research methodologies were applied to achieve the stated objective of the study. The rough surface of the object was modeled using numerical scheme generating Gaussian rough surface with isotropic surface texture. Random rough surface was generated using the most efficient way to perform filtering operations which is FFT to generate point clouds in a space. The point clouds were converted into three-dimensional (3D) models using SolidWorks software. Furthermore, the generated random rough surface was imported to a commercial FEM software called Abaqus to simulate static contact on a rough surface. Mesh independent test were performed to show the independence of the computational result on the generated mesh of the model.

The simulation result of the study for contact characteristics including the maximum von mises stress, the contact pressure distribution and the real contact area at different load level are analyzed. By evaluating the total area of contact on Abaqus as a proportion of the surface's area, the dimensionless area of contact was determined. This proportional area was taken to be equal to the nominal contact area for the entire surface. At each applied load level, the relative contact area, Ar/A, was calculated by averaging the measurements from Abaqus. The load is normalized by dividing by nominal area of contact and the elastic modulus (E`). Finally, several conclusions can be drawn as follows:

Result of the study for the variation of dimensionless real area of contact with dimensionless contact load for both PM surface model and machined surface model with varying surface finishing showed that; as the dimensionless contact load increases, the number of contact point and the dimensionless real area of contact also increases in a nonlinear or exponential manner. Result of dimensionless mean contact pressure with the dimensionless contact load for the same dimensionless contact load, the PM surface finish surface shows a relatively higher mean contact pressure compared to machined surface finish rough surface.

The numerical result for the variation of dimensionless maximum contact pressure with dimensionless contact load for both the rough surface contact model observation shows that when the average roughness decreases, the required dimensionless contact load to cross the hardness limit increases.

This study result is in lined with the result noted in Bhushan [24], where there is an increasing trend in the maximum contact pressure beyond the hardness limit for various applied loads. The machined surface finish rough surface model reaches the hardness limit earlier compared to the PM surface finish rough surface model because in the former rough surface model (PM surface finish), the contacting area is small and the asperities are severe plastic deformation. In the PM surface model, the $P_{\max}/Y$ ratio to cross the hardness limit of 2.22 at $P_n/A_n E$ of 0.0042 and in the machined surface model the $P_{\max}/Y$ ratio to cross the hardness limit of 2.22 at $P_n/A_n E$ of 0.0057. Furthermore, the computational result of the effect of surface finish method on the von Mises stress and the contact pressure distribution plot shows that the machined surface has more asperity interaction compared to PM surface at the same contact load.

The result for the effect of material density variation for PM surface were also computed. The variation of dimensionless real area of contact with dimensionless applied contact load for both the rough surface depicted that both real area of contact and total number of contact points increase in a nonlinear with dimensionless normal contact load increase. Variation of dimensionless mean contact pressure with the dimensionless contact load for rough surface contact models with varying material density were also analyzed and the result revealed that as the contact load increase, the mean contact pressure increases and the mean contact pressure increases as the material density decrease. The real contact area is low and the von mises stresses and contact pressure are high for the low-density surface with $\rho = 7.35 g/cm^3$ as compared to high-density surface with $\rho = 7.55 g/cm^3$. For the surface with $\rho = 7.35 g/cm^3$, real contact area occurs at $0.6377 mm^2$ or 10.2% of nominal contact area, the maximum von mises stress value is 1578MPa and maximum contact pressure value is 2804MPa. For the surface with $\rho = 7.35 g/cm^3$, real contact area occurs at 1.14115 mm^2 or 18.25% of nominal contact area, the maximum von mises stress value is 878.3MPa and maximum contact pressure value is 1266 MPa.

The simulation result for variation of dimensionless maximum contact pressure with the dimensionless contact load for rough surface having two different material density showed that each rough surface contact model reaches its hardness limit at a different dimensionless contact load. The high-density rough surface model reaches the hardness limit earlier compared to the low-density rough surface model High density model shows a greater number of asperity contacts and low asperity interaction compared to low density model.

5.2 Recommendations

- To attain the same dimensionless real area of contact, PM surface has to take additional contact load due to large average roughness value even though the number of asperities is high. Thus, to obtain low pressure between contacting bodies, using machined surface could be more applicable relative to PM surface finish.
- The relationship between real area of contact, average contact pressure and maximum contact pressure with applied normal load is consistent with what is commonly observed in engineering practice. Therefore, by utilizing a smoother surface finishing technique, plastic deformation can be avoided.
- For the same dimensionless contact load, the higher density surface shows a relatively high real contact area compared to low density surface. Due to small value of average roughness and high elastic modulus, rough surface having large size of asperities and also exhibits high dimensionless real area of contact. Thus, to attain the same dimensionless real area of contact, lower density surface has to take additional contact load due to large average roughness value and lower elastic modulus value.
- Use the integration of mathematical, CAD and FE software can be develop 3D rough surface mode to investigate the contact parameters (real contact area, and contact pressure) of two bodies under the application of load effectively.
- Studying of contact parameters in different density and surface finish with varying load is helpful to study about contact fatigue, wear and metal defect (crack) analysis.

5.2.1 Future work

- The analysis of Gaussian rough surface interactions with the assumption of completely plastic deformation is the exclusive focus of the current study. It is also possible to extend the same study to rough surface contacts that exhibit strain hardening behavior.

- Contact fatigue behavior of carburized moly based low alloy with different density and surface finish.
- The effect of the surface roughness on the crack initiation and propagation.

References

[1] M. F. AL-Mayali, “Plastic Deformation and Residual Stress of Surface Roughness Asperities in Elastohydrodynamic Contact with Consideration of Surface Fatigue by Maasi F . AL-Mayali Thesis submitted in candidature for the degree of Doctor of Philosophy at Cardiff University,” 2017.

[2] P. L. Menezes, S. P. Ingole, M. Nosonovsky, S. V. Kailas, and M. R. Lovell, *Tribology for scientists and engineers: From basics to advanced concepts*, vol. 9781461419, no. November. 2013.

[3] Y. Zhang, “The effect of surface roughness parameters on contact and wettability of solid surfaces,” 2007. [Online]. Available: http://lib.dr.iastate.edu/rtd

[4] H. Bhushan, *Introduction to tribology.*, Second. New Delhi: John Wiley & Sons, Ltd, 2013.

[5] J. P. Davim, “A note on the determination of optimal cutting conditions for surface finish obtained in turning using design of experiments,” *J. Mater. Process. Technol.*, vol. 116, no. 2–3, pp. 305–308, 2001.

[6] H. Zein and O. M. Irfan, “Surface roughness investigation and stress modeling by finite element on orthogonal cutting of copper,” *Metals (Basel).*, vol. 8, no. 6, 2018.

[7] X. Guo, B. Ma, and Y. Zhu, “A magnification-based multi-asperity (MBMA) model of rough contact where the Greenwood-Williamson and Persson theories meet,” *J. Mech. Phys. Solids*, pp. 1–53, 2017.

[8] J. Timur, G. Anyar, G. A. Sipayung, R. Ismail, J. Jamari, and A. P. Bayuseno, “Finite Element Method for Modeling,” vol. 11, no. 7, pp. 134–149, 2020.

[9] C. Alamsyah, S. A. Dillich, and A. P. Femia, “Effects of initial surface finish on CAM wear,” *Wear Mater. Int. Conf. Wear Mater.*, vol. 134, pp. 657–664, 1989.

[10] T. V. Vorbuguer, “Surface finish metrology tutorial,” *National Institute of Standards and Technology*. pp. 1–159, 1990. [Online]. Available: https://www.nist.gov/system/files/documents/calibrations/89-4088.pdf

[11] H. A. Rothbart, *Cam Design Handbook*, First. New York: McGRAW-HILL, 2004.

[12] T. H. C. Childs, “Review of wear control handbook,” *Tribology International*, vol. 14, no. 5.

pp. 255–256, 1981.

[13] A. Misra, "Mechanistic Model for Contact between Rough Surfaces," *J. Eng. Mech.*, vol. 123, no. 5, pp. 475–484, 1997.

[14] A. J. Makadia and J. I. Nanavati, "Optimisation of machining parameters for turning operations based on response surface methodology," *Meas. J. Int. Meas. Confed.*, vol. 46, no. 4, pp. 1521–1529, 2013.

[15] H. Hatem, "Study the Effect of Cutting Conditions for turning process on the Machined Surface," *Coll. Eng. J.*, vol. 14, no. 1, p. 61, 2011.

[16] Kartini, E. Saputra, R. Ismail, J. Jamari, and A. P. Bayuseno, "Analysis of the contact area of smooth and rough surfaces in contact with sphere indenter using finite element method," in *MATEC Web of Conferences*, 2016, vol. 58, pp. 1–5.

[17] A. Torabi, S. Akbarzadeh, M. R. Salimpour, and M. Taei, "Effect of surface roughness pattern on transient mixed elastohydrodynamic lubrication," *Surf. Topogr. Metrol. Prop.*, vol. 4, no. 1, 2016.

[18] T. ul Islam, M. Khurram, M. Umar, R. A. Mufti, and K. Akhtar, "Experimental and theoretical evaluation of friction in roller follower valve train," *Meas. J. Int. Meas. Confed.*, vol. 160, p. 107808, 2020.

[19] H. BAŞ, "Investigation of effects of surface roughness on the performance of cam mechanisms," *Int. J. Automot. Eng. Technol.*, pp. 67–73, 2021.

[20] H. Hertz, "H. Hertz, Über die Berührung fester elastischer Körper, Journal für die reine und angewandte Mathematik 92, 156-171 (1881)," *J. für die reine und Angew. Math.*, vol. 171, pp. 156–171, 1881.

[21] R. Ismail, "Running-in of Rolling-sliding Contacts," University of Twente, 2013.

[22] S. Tesfaye Mekonone, W. Pahl, and A. Molinari, "Influence of the microstructure on the subsurface and surface damage during lubricated rolling–sliding wear of sintered and sinterhardened 1.5%Mo–2%Cu–0.6%C steel: theoretical analysis and experimental investigation," Taylor & Francis, 2018.

[23] J. A. Greenwood; J. B. P. Williamson, "Contact of nominally flat surfaces," *Proc. R. Soc.*

London. Ser. A. Math. Phys. Sci., vol. 295, no. 1442, pp. 300–319, 1966.

[24] B. Bhushan, "Contact mechanics of rough surfaces in tribology: Multiple asperity contact," *Tribol. Lett.*, vol. 4, no. 1, pp. 1–35, 1998.

[25] P. B. Abel and J. Ferrante, *Modern Triboly Handbook*, First. Ohio: CRC Press LLC, 2001.

[26] D. J. Whitehouse and J. F. Archard, "The properties of random surfaces of significance in their contact," *Proc. R. Soc. London. A. Math. Phys. Sci.*, vol. 316, no. 1524, pp. 97–121, 1970.

[27] R. A. Onions and J. F. Archard, "The contact of surfaces having a random structure," *J. Phys. D. Appl. Phys.*, vol. 6, no. 3, pp. 289–304, 1973.

[28] A. W. Bush, R. D. Gibson, and T. R. Thomas, "The elastic contact of a rough surface," *Wear*, vol. 35, no. 1, pp. 87–111, 1975.

[29] T. Hisakado, "Effect of surface roughness on contact between solid surfaces," *Wear*, vol. 28, no. 2, pp. 217–234, 1974.

[30] J. I. McCool, "Comparison of models for the contact of rough surfaces," *Wear*, vol. 107, no. 1, pp. 37–60, 1986.

[31] J. A. Greenwood and J. B. P. Williamson, "Contact of nominally flat surfaces," *Proc. R. Soc. London. Ser. A. Math. Phys. Sci.*, vol. 295, no. 1442, pp. 300–319, 1966.

[32] A. W. Bush and G. P. Keogh, "Strongly anisotropic rough surfaces," *J. Tribol.*, vol. 101, no. 1, pp. 15–20, 1979.

[33] V. A. Yastrebov, J. Durand, H. Proudhon, and G. Cailletaud, "Rough surface contact analysis by means of the Finite Element Method and of a new reduced model," *Comptes Rendus - Mec.*, vol. 339, no. 7–8, pp. 473–490, 2011.

[34] J. Jamari and D. J. Schipper, "Deterministic repeated contact of rough surfaces," *Wear*, vol. 264, no. 3–4, pp. 349–358, 2008.

[35] J. Jamari and D. J. Schipper, "Experimental investigation of fully plastic contact of a sphere against a hard flat," *J. Tribol.*, vol. 128, no. 2, pp. 230–235, 2006.

[36] K. L. Johnson, *Contact Mechanics*, First. Cambridge: Cambridge University Press, 1985.

[37] P. Ranganath Nayak, "Random process model of rough surfaces," *J. Tribol.*, vol. 93, no. 3, pp.

398–407, 1971.

[38] G. Yang, B. Li, Y. Wang, and J. Hong, “Numerical simulation of 3D rough surfaces and analysis of interfacial contact characteristics,” *C. - Comput. Model. Eng. Sci.*, vol. 103, no. 4, pp. 251–279, 2014.

[39] U. G. Movement, H. Area, and P. Review, “Appendix ‘ B ’ Appendix ‘ B ,’” *Civ. hope how ordinary Am. keep Democr. alive*, vol. 6, no. c, pp. 401–402, 2018.

[40] H. Shimodaira, “Gaussians,” vol. 2, no. ii, 2020, pp. 1–9.

[41] Z. Hongwei, Z. Xuehua, and Z. Bao’an, “System Dynamics Approach to Urban Water Demand Forecasting,” *Trans. Tianjin Univ.*, vol. 15, no. 1, pp. 70–74, 2009.

[42] A. Gherbi and M. Belgasmia, *Stochastic analysis basics and application of statistical linearization technique on a controlled system with nonlinear viscous dampers*. Elsevier Inc., 2019.

[43] C. Van Valkenburg, O. F. Receitly, and I. Radiation-resistant, “Redacted for privacy Redacted for privacy Redactéd for privacy,” 1959.

[44] D . J . Wliitehouse, “THE PROPERTIES OF RANDOM SURFACES,” 1971.

[45] Y. Z. Hu and K. Tonder, “Simulation of 3-D random rough surface by 2-D digital filter and fourier analysis,” *Int. J. Mach. Tools Manuf.*, vol. 32, no. 1–2, pp. 83–90, 1992.

[46] Q. Tao, H. P. Lee, and S. P. Lim, “Contact mechanics of surfaces with various models of roughness descriptions,” *Wear*, vol. 249, no. 7, pp. 539–545, 2001.

[47] L. Pei, S. Hyun, J. F. Molinari, and M. O. Robbins, “Finite element modeling of elasto-plastic contact between rough surfaces,” *J. Mech. Phys. Solids*, vol. 53, no. 11, pp. 2385–2409, 2005.

[48] M. Soejima, E. Ogawa, M. Nagafuji, and T. Kuwahara, “Influence of cam surface finish and roughness on frictional power loss in valve trains with roller tappets,” in *Proceedings of the World Tribology Congress III - 2005*, 2005, pp. 581–582.

[49] D. Y. Hua, K. Farhang, and L. E. Seitzman, “A multi-scale system analysis and verification for improved contact fatigue life cycle of a cam-roller system,” *J. Tribol.*, vol. 129, no. 2, pp. 321–325, 2007.

[50] Z. Jiang *et al.*, “Study on surface roughness muring metal manufacturing process,” *Adv. Mater.*

Res., vol. 325, pp. 731–736, 2011.

[51] G. Pawar, P. Pawlus, I. Etsion, and B. Raeymaekers, "The effect of determining topography parameters on analyzing elastic contact between isotropic rough surfaces," *J. Tribol.*, vol. 135, no. 1, pp. 1–10, 2013.

[52] P. H. Nilsson, "Tribological Aspect of the Surface," in *Tribological Aspect of the Surface*, 2014, no. July 2008.

[53] A. Megalingam and M. M. Mayuram, "Effect of surface parameters on finite element method based deterministic Gaussian rough surface contact model," *Proc. Inst. Mech. Eng. Part J J. Eng. Tribol.*, vol. 228, no. 12, pp. 1358–1373, 2014.

[54] L. S. Yousuf and N. H. Hadi, "Contact Stress Distribution of a Pear Cam Profile with Roller Follower Mechanism," *Chinese J. Mech. Eng. (English Ed.*, vol. 34, no. 1, 2021.

[55] P. Sahoo and B. Chatterjee, "A Finite Element Study of Elastic-Plastic Hemispherical Contact Behavior against a Rigid Flat under Varying Modulus of Elasticity and Sphere Radius," *Engineering*, vol. 02, no. 04, pp. 205–211, 2010.

[56] S. Shankar and M. M. Mayuram, "A finite element based study on the elastic-plastic transition behavior in a hemisphere in contact with a rigid flat," *J. Tribol.*, vol. 130, no. 4, pp. 1–6, 2008.

[57] S. Sahatwitter and R. L. Jackson, "Elastic and elastic-perfectly plastic analysis of an axisymmetric sinusoidal surface asperity contact surface asperity contact," *Tribol. - Mater. Surfaces Interfaces*, vol. 0, no. 0, pp. 1–21, 2019.

[58] S. T. Mekonone, "Theoretical analysis and experimental investigation of contact fatigue and surface damage in prealloyed and diffusion bonded sintered steels," University of Trento, 2018.

[59] J. J. Wu, "Simulation of rough surfaces with FFT," *Tribol. Int.*, vol. 33, no. 1, pp. 47–58, 2000.